Inorganic Chemistry

ARTICLE

pubs.acs.org/IC

Comparison of Structure and Reactivity of Phosphine-Amido and Hemilabile Phosphine-Amine Chelates of Rhodium

Lindsay J. Hounjet,[†] Robert McDonald,[‡] Michael J. Ferguson,[‡] and Martin Cowie*[,†]

[†]Department of Chemistry and [‡]X-ray Crystallography Laboratory, University of Alberta, Edmonton, Alberta T6G 2G2, Canada

Supporting Information

ABSTRACT:

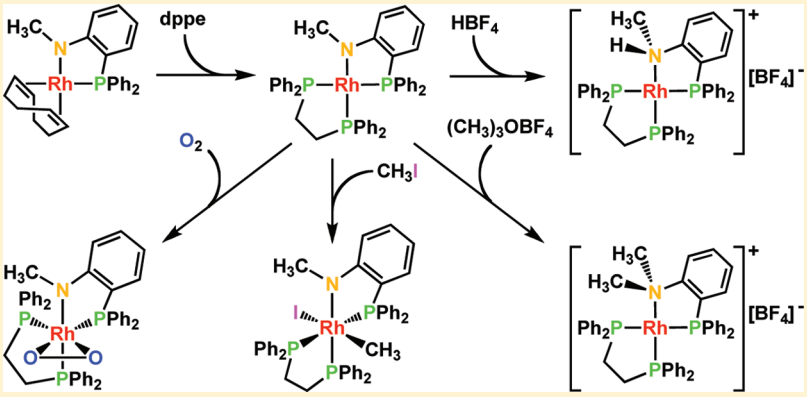

A series of mono- and binuclear rhodium(I) complexes bearing *ortho*-phosphinoanilido and *ortho*-phosphinoaniline ligands has been synthesized. Reactions of the protic monophosphinoanilines, Ph_2PAr or $PhPAr_2$ (Ar = *o*-C_6H_4NHMe), with 0.5 equiv of $[Rh(\mu\text{-OMe})(COD)]_2$ result in the formation of the neutral amido complexes, $[Rh(COD)(P,N\text{-}Ph_2PAr^-)]$ or $[Rh(COD)(P,N\text{-}PhP(Ar^-)Ar)]$ (Ar^- = *o*-$C_6H_4NMe^-$), respectively, through stoichiometrically controlled deprotonation of an amine by the internal methoxide ion. Similarly, the binuclear complex, $[Rh_2(COD)_2(\mu\text{-}P,N,P',N'\text{-mapm}^{2-})]$ ($mapm^{2-}$ = $Ar(Ar^-)PCH_2P(Ar^-)Ar$), can be prepared by reaction of the protic diphosphinoaniline, mapm ($Ar_2PCH_2PAr_2$), with 1 equiv of $[Rh(\mu\text{-OMe})(COD)]_2$. An analogous series of hemilabile phosphine-amine compounds can be generated by reactions of monophosphinoanilines, Ph_2PAr' or $PhPAr'_2$ (Ar′ = *o*-$C_6H_4NMe_2$), with 1 equiv of $[Rh(NBD)_2][BF_4]$ to generate $[Rh(NBD)(P,N\text{-}Ph_2PAr')][BF_4]$ or $[Rh(NBD)(P,N\text{-}PhPAr'_2)][BF_4]$, respectively, or by reactions of diphosphinoanilines, mapm or dmapm ($Ar'_2PCH_2PAr'_2$), with 2 equiv of the rhodium precursor to generate $[Rh_2(NBD)_2(\mu\text{-}P,N,P',N'\text{-mapm})][BF_4]_2$ or $[Rh_2(NBD)_2(\mu\text{-}P,N,P',N'\text{-dmapm})][BF_4]_2$, respectively. Displacement of the diolefin from $[Rh(COD)(P,N\text{-}Ph_2PAr^-)]$ by 1,2-bis(diphenylphosphino)ethane (dppe) yields $[Rh(P,P'\text{-dppe})(P,N\text{-}Ph_2PAr^-)]$ which, while unreactive to H_2, reacts readily and irreversibly with oxygen to form the peroxo complex, $[RhO_2(P,P'\text{-dppe})(P,N\text{-}Ph_2PAr^-)]$, and with iodomethane to yield $[RhI(CH_3)(P,P'\text{-dppe})(P,N\text{-}Ph_2PAr^-)]$. Hemilabile phosphine-amine compounds can also be prepared by reactions of $[Rh(P,P'\text{-dppe})(P,N\text{-}Ph_2PAr^-)]$ with Me_3OBF_4 or $HBF_4\cdot Et_2O$, resulting in (thermodynamic) additions at nitrogen to form $[Rh(P,P'\text{-dppe})(P,N\text{-}Ph_2PAr')][BF_4]$ or $[Rh(P,P'\text{-dppe})(P,N\text{-}Ph_2PAr)][BF_4]$, respectively. The nonlabile phosphine-amido and hemilabile phosphine-amine complexes were tested as catalysts for the silylation of styrene. The amido species do not require the use of solvents in reaction media, can be easily removed from product mixtures by protonation, and appear to be more active than their hemilabile, cationic congeners. Reactions catalyzed by either amido or amine complexes favor dehydrogenative silylation in the presence of excess olefin, showing modest selectivities for a single vinylsilane product. The binuclear complexes, which were prepared in an effort to explore possible catalytic enhancements of reactivity due to metal−metal cooperativity, are in fact somewhat less active than mononuclear species, discounting this possibility.

INTRODUCTION

The rich and varied chemistry of transition metal complexes bearing chelating, bifunctional ligands includes the development of increasingly efficient and unique homogeneous catalytic systems.[1−11] Within metal complexes, these bifunctional hybrid ligands are known to exhibit hemilability, whereby at least one of the donors is strongly coordinating and anchored to the metal, while the more labile donor(s) can be displaced by catalytic substrates, but can also offer chelate stabilization in the event of coordinative unsaturation.[12−17] Low-valent, late transition metals, which form strong bonds with softer phosphines and

Received: September 14, 2010
Published: May 17, 2011

weak bonds with harder amines are commonly ligated by phosphine-amines to generate hemilabile complexes.[18−25] Furthermore, the use of incompletely *N*-substituted amine donors within such hybrid *P,N*-ligands allows for deprotonation of the coordinated amines to generate nonlabile phosphine-amido complexes, some of which have found catalytic applications.[26−30] Late-metal amido complexes (particularly of ruthenium) are widely used as catalysts for the hydrogenation of polar unsaturates whereby dihydrogen heterolysis is achieved through metal−ligand cooperativity to generate hydrido-amine complexes, which can then undergo hydride and proton transfer to the substrate via an outer-sphere, bifunctional mechanism.[8,31−33]

In earlier studies involving a series of hybrid *P,N*-ligands based on *ortho*-phosphinoanilines, we investigated mono- and binuclear complexes of rhodium in which the degree of methyl substitution at nitrogen was found to have a significant influence on both structure and hemilability.[22] In related chemistry with ruthenium, the structural diversity was again demonstrated in which alteration of the *N*-donor was found to give rise to a number of different coordination modes,[26] although the hemilability observed at rhodium was not exhibited by these ruthenium complexes. One of our primary interests in the protic *ortho*-phosphinoaniline ligands was the possibility for deprotonation of the amine groups to yield phosphine-amido chelates, the reactivity of which could then be compared to the phosphine-amine analogues. In keeping with the well established reactivity of amido complexes (particularly involving ruthenium)[31−33] one of our phosphine-amido complexes was found to be active as a ketone transfer hydrogenation catalyst.[26] In the current study, we set out to extend our original investigation of phosphine-amine complexes of rhodium and to compare their reactivities with those of the related phosphine-amido species.

To compare the reactivity of amido and amine complexes we targeted the silylation of olefins, for which rhodium is known to be effective.[11,34,35] The hydrosilylation of organic reagents to generate organosilanes has many potential applications for the production of new electronic materials and polymers.[36] Olefin hydrosilylation catalyzed by late metal complexes is often accompanied by dehydrogenative silylation side-reactions, particularly when rhodium is the metal used.[11,34,35] However, the selective formation of unsaturated organosilicon compounds could be useful for generating a variety of functionalized silanes by subjecting the alkene functionality of the product vinylsilane to further substrate addition. The possibility of metal−metal cooperativity in reactions catalyzed by amido or amine complexes prompted us to prepare binuclear complexes and to compare their reactivities with those of the mononuclear analogues.

EXPERIMENTAL SECTION

General Comments. All solvents were deoxygenated, dried (using appropriate drying agents), distilled before use, and stored under nitrogen. Unless indicated otherwise, all reactions were performed under an Ar atmosphere using standard Schlenk techniques. The reagents, diphenyl(*o*-*N*-methylanilinyl)phosphine (Ph_2PAr),[22] di(*o*-*N*-methylanilinyl)phenylphosphine ($PhPAr_2$),[22] bis(di(*o*-*N*-methylanilinyl)phosphino)methane (mapm),[22] diphenyl(*o*-*N*,*N*-dimethylanilinyl)phosphine (Ph_2PAr'),[37] bis(*o*-*N*,*N*-dimethylanilinyl)phenylphosphine ($PhPAr'_2$),[37] bis(di(*o*-*N*,*N*-dimethylanilinyl)phosphino)methane (dmapm)[38] and $[Rh(\mu\text{-OMe})(COD)]_2$[39] were prepared according to literature procedures. Styrene (≥99%, deoxygenated and stored under Ar over 4 Å molecular sieves), trifluoromethanesulfonic acid (HOTf; ≥ 99%, stored under Ar), hydrogen tetrafluoroborate (HBF_4; 54% (w/w) in Et_2O, stored under Ar), iodomethane (99.5%), trimethyloxonium tetrafluoroborate (Me_3OBF_4; 95%), and 1,2-bis(diphenylphosphino)ethane (dppe; 97%) were purchased from Aldrich. Triethylsilane ($HSiEt_3$; ≥ 98%, deoxygenated and stored under Ar over 4 Å molecular sieves) was purchased from Alfa-Aesar while $[Rh(NBD)_2][BF_4]$ (≥ 96%, stored under Ar) was purchased from Strem Chemicals. NMR spectra were recorded on Varian Inova-400, -500, or Varian Unity-500 spectrometers operating at 399.8, 498.1, or 499.8 MHz, respectively, for ^1H, at 161.8, 201.6, or 202.3 MHz, respectively, for ^{31}P and at 100.6, 125.3, or 125.7 MHz, respectively, for ^{13}C nuclei. Coupling constants are given in Hz. Overlapping or unresolved aromatic ^1H signals, observed in the typical δ 6−8 range, and aromatic $^{13}C\{^1H\}$ signals, found between δ 80−120, are not reported. Spectroscopic data for metal complexes (**1a**−**9**) are provided in Table 1. Elemental analyses were performed by the Microanalytical Laboratory of this department. Electrospray ionization mass spectra were run on a Micromass Zabspec spectrometer in the departmental MS facility. In all cases, the distribution of isotope peaks for the appropriate parent ion matched very closely that calculated from the formulation given.

Preparation of Metal Complexes. *(a) η^2:η^2-1,5-Cyclooctadiene(P,N-diphenyl(o-N-methylanilido)phosphine)rhodium(I), [Rh(COD)(P,N-Ph$_2$PAr$^-$)] (**1a**).* In a 100 mL Schlenk flask under anhydrous conditions and Ar atmosphere, Ph_2PAr (768 mg, 2.64 mmol) and $[Rh(\mu\text{-OMe})(COD)]_2$ (638 mg, 1.32 mmol) were dissolved in 10 mL of benzene at ambient temperature resulting in a brilliant red-orange solution. The solvent volume was reduced to approx 5 mL in vacuo, and 20 mL of *n*-pentane was then added resulting in the formation of an orange precipitate. The slurry was stirred for 10 min before allowing the precipitate to settle. The supernatant was removed by cannula transfer under Ar, then the solid was dried in vacuo and recovered as an orange powder (1.13 g, 74% yield, found: C, 66.67; H, 5.97; N, 2.59%. Calcd for $[C_{27}H_{29}NPRh]\cdot 0.5C_6H_6$: C, 66.96; H, 6.02; N, 2.75%). Although the crystal structure indicates 1 equiv of benzene per formula unit, a noncrystalline sample was analyzed here and ^1H NMR analysis in CD_2Cl_2 (obtained at approximately the same time as the elemental analysis) was used to verify benzene content. Single crystals suitable for X-ray diffraction were obtained by layering a saturated benzene solution with *n*-pentane in an NMR tube.

*(b) η^2:η^2-1,5-Cyclooctadiene(P,N-((o-N-methylanilido)(o-N-methylanilinyl)phenylphosphine))rhodium(I), [Rh(COD)(P,N-PhP(Ar$^-$)Ar)] (**1b**).* The compound was prepared in a manner similar to that of **1a** using $PhPAr_2$ (224 mg, 698 μmol) and $[Rh(\mu\text{-OMe})(COD)]_2$ (169 mg, 349 μmol) and was isolated as a red-orange powder (220 mg, 59% yield, found: C, 63.55; H, 6.00; N, 5.20%. Calcd for $[C_{28}H_{32}N_2PRh]$: C, 63.40; H, 6.08; N, 5.28%). HRMS (ESI): *m*/*z* 531.1432 $[M + H]^+$. Calcd for $C_{28}H_{33}N_2PRh$: *m*/*z* 531.1431.

*(c) bis(η^2:η^2-1,5-Cyclooctadiene)(μ-P,N,P′,N′-di((o-N-methylanilido)-(o-N-methylanilinyl)phosphino)methane)dirhodium(I,I), [Rh$_2$(COD)$_2$-(μ-P,N,P′,N′-mapm^{2-})] (**2**). Method a.* In a 50 mL Schlenk tube under anhydrous conditions and Ar atmosphere, mapm (71 mg, 142 μmol) and $[Rh(\mu\text{-OMe})(COD)]_2$ (68 mg, 140 μmol) were dissolved in 2 mL of tetrahydrofuran at ambient temperature resulting in a dark red solution. To the stirred solution was then added 10 mL of *n*-pentane, which resulted in the formation of an orange precipitate. The slurry was stirred for 10 min before allowing the precipitate to settle. The supernatant was removed by cannula transfer under Ar, then the solid was dried in vacuo and recovered as an orange powder (99 mg, 71% yield, found: C, 59.13; H, 6.58; N, 5.43%. Calcd for $[C_{45}H_{56}N_4P_2Rh_2]\cdot C_4H_8O$: C, 59.28; H, 6.50; N, 5.64%). Single crystals suitable for X-ray diffraction were obtained by slow evaporation from a tetrahydrofuran solution in an NMR tube. *Method b.* The reaction above was also carried out using 5 mL of benzene rather than 2 mL of tetrahydrofuran, and in this case, a red slurry was immediately produced rather than a dark red solution. Product isolation was identical to that of *Method a.*

Table 1. NMR Spectroscopic Data for the Compounds[a]

compound	$\delta(^{31}P\{^1H\})$/ppm[b]	$\delta(^1H)$/ppm[c]	$\delta(^{13}C\{^1H\})$/ppm[c]
[Rh(COD)(*P*,*N*-Ph_2PAr^-)] (**1a**)	41.2 (d, $^1J_{RhP}$ = 163 Hz, 1P)[d]	H_{COD}: 5.26 (m/br, 2H), 3.33 (m/br, 2H), 2.13 (m/br, 4H), 1.82 (m/br, 4H)[d] RhNCH_3: 2.94 (s, 3H)[d]	RhNCH_3: 39.1 (s)[d]
[Rh(COD)(*P*,*N*-PhP(Ar^-)Ar)] (**1b**)	25.9 (d, $^1J_{RhP}$ = 157 Hz, 1P)[d]	N*H*: 6.95 (m/br, 1H)[d] H_{COD}: 5.31 (m/br, 1H), 5.10 (m/br, 1H), 3.29 (m/br, 2H), 1.92 (m/br, 8H)[d] RhNCH_3: 2.93 (s, 3H)[d] HNCH_3: 2.43 (d, $^3J_{HH}$ = 4.4 Hz, 3H)[d]	RhNCH_3: 39.0 (s)[d] HNCH_3: 29.0 (s)[d]
[Rh_2(COD)$_2$(μ-*P*,*N*,*P*′,*N*′-mapm^{2-})] (**2**)	11.7 (m, $^1J_{RhP}$ = 165 Hz, 2P)[d,e]	*H*NCH_3: 6.51 (m/br, 2H)[d,e] H_{COD}: 5.27 (m, 2H), 4.66 (m, 2H), 2.97 (m, 2H), 2.74 (m, 2H), 2.31 (m, 2H), 2.05 (m, 4H), 1.84 (m, 4H), 1.55 (m, 6H)[d,e] PCH_2P: 3.17 (t, $^2J_{PH}$ = 10.0 Hz, 2H)[d,e] RhNCH_3: 2.63 (s, 6H)[d,e] HNCH_3: 2.34 (d, $^3J_{HH}$ = 5.2 Hz, 6H)[d,e]	RhNCH_3: 39.1 (s)[d,e] HNCH_3: 30.4 (s)[d,e] PCH_2P: 18.9 (t, $^1J_{PC}$ = 17 Hz)[d,e]
[Rh(*P*,*P*′-dppe)(*P*,*N*-Ph_2PAr^-)] (**3**)	67.9 (ddd, $^1J_{RhP}$ = 142 Hz, $^2J_{PP}$ = 37 Hz, $^2J_{PP}$ = 33 Hz, 1P),[f] 59.0 (ddd, $^1J_{RhP}$ = 159 Hz, $^2J_{PP}$ = 312 Hz, $^2J_{PP}$ = 33 Hz, 1P),[f] 46.0 (ddd, $^1J_{RhP}$ = 143 Hz, $^2J_{PP}$ = 312 Hz, $^2J_{PP}$ = 37 Hz, 1P)[f]	NCH_3: 2.93 (s, 3H)[f] P(CH_2)$_2$P: 2.00 (m, 4H)[f]	NCH_3: 47.0 (d, $^3J_{PC}$ = 12 Hz)[f] P(CH_2)$_2$P: 30.2 (m) 26.3 (m)[f]
[RhO_2(*P*,*P*′-dppe)(*P*,*N*-Ph_2PAr^-)] (**4**)	52.3 (ddd, $^1J_{RhP}$ = 130 Hz, $^2J_{PP}$ = 20 Hz, $^2J_{PP}$ = 9 Hz, 1P), 50.8 (ddd, $^1J_{RhP}$ = 134 Hz, $^2J_{PP}$ = 13 Hz, $^2J_{PP}$ = 9 Hz, 1P), 41.0 (ddd, $^1J_{RhP}$ = 106 Hz, $^2J_{PP}$ = 20 Hz, $^2J_{PP}$ = 13 Hz, 1P)	NCH_3: 2.91 (d, $^4J_{PH}$ = 4.4 Hz, 3H) P(CH_2)$_2$P: 2.11 (m, 4H)	N/A (decomposes in CD_2Cl_2; poor solubility in other solvents)
[RhI(CH_3)(*P*,*P*′-dppe)(*P*,*N*-Ph_2PAr^-)] (**5**)	49.2 (ddd, $^1J_{RhP}$ = 107 Hz, $^2J_{PP}$ = 445 Hz, $^2J_{PP}$ = 25 Hz, 1P),[d] 38.0 (ddd, $^1J_{RhP}$ = 101 Hz, $^2J_{PP}$ = 445 Hz, $^2J_{PP}$ = 12 Hz, 1P)[d] 36.7 (dm, $^1J_{RhP}$ = 102 Hz, 1P)[d]	P(CH_2)$_2$P: 3.60 (m, 1H), 2.68 (m, 1H), 2.47 (m, 1H), 2.02 (m, 1H)[d] NCH_3: 3.41 (s, 3H)[d] RhCH_3: 0.79 (d, $^2J_{RhH}$ = 2.0 Hz, 3H)[d]	NCH_3: 49.9 (d, $^2J_{RhC}$ = 6 Hz)[d] P(CH_2)$_2$P: 31.8 (m) 26.9 (m)[d] RhCH_3: 13.2 (m, $^1J_{RhC}$ = 22 Hz)[d]

dx.doi.org/10.1021/ic101883u |*Inorg. Chem.* 2011, 50, 5361–5378

Table 1. Continued

compound	$\delta(^{31}P\{^{1}H\})$/ppm[b]	$\delta(^{1}H)$/ppm[c]	$\delta(^{13}C\{^{1}H\})$/ppm[c]
[Rh(*P*,*P*′-dppe)(*P*,*N*-Ph_2PAr')][BF_4] (**6**)	69.2 (ddd, $^{1}J_{RhP}$ = 130 Hz, $^{2}J_{PP}$ = 35 Hz, $^{2}J_{PP}$ = 31 Hz, 1P), 55.0 (ddd, $^{1}J_{RhP}$ = 149 Hz, $^{2}J_{PP}$ = 291 Hz, $^{2}J_{PP}$ = 31 Hz, 1P), 43.1 (ddd, $^{1}J_{RhP}$ = 142 Hz, $^{2}J_{PP}$ = 291 Hz, $^{2}J_{PP}$ = 35 Hz, 1P)	$N(CH_3)_2$: 3.03 (s, 6H) $P(CH_2)_2P$: 2.06 (m, 4H)	N/A
[Rh(NBD)(*P*,*N*-Ph_2PAr')][BF_4] (**7a**)	37.7 (d, $^{1}J_{RhP}$ = 177 Hz, 1P)	H_{NBD}: 5.62 (s/br, 2H), 4.12 (s/br, 4H), 1.72 (m/br, 2H) $N(CH_3)_2$: 3.02 (s, 6H) H_{NBD}: 5.56 (s/br, 2H), 4.05 (s/br, 2H), 4.02 (s/br, 2H), 1.66 (d, $^{2}J_{HH}$ = 8.8 Hz, 1H), 1.60 (d, $^{2}J_{HH}$ = 8.8 Hz, 1H)[h] $N(CH_3)_2$: 2.94 (s, 6H)[h]	$N(CH_3)_2$: 52.3 (s)
[Rh(NBD)(*P*,*N*-$PhPAr'_2$)][BF_4] (**7b**)	27.5 (d, $^{1}J_{RhP}$ = 171 Hz, 1P)	H_{NBD}: 4.49 (s/br, 4H), 4.00 (s/br, 2H), 1.62 (s/br, 2H) $N(CH_3)_2$: 2.84 (s, 12H)	$N(CH_3)_2$: 50.4 (s)
[Rh_2(NBD)$_2$(*μ*-*P*,*N*,*P*′,*N*′-dmapm)][BF_4]$_2$ (**8**)	12.0 (m, $^{1}J_{RhP}$ = 180 Hz, 2P)[e] 9.7 (m/br, $^{1}J_{RhP}$ = 177 Hz, 2P)[e,h] 7.4 (m/br, $^{1}J_{RhP}$ = 183 Hz, 2P)[g,h]	H_{NBD}: 5.40 (s/br, 4H), 3.76 (s, 4H), 3.40 (s/br, 4H), 1.50 (s, 4H)[e] PCH_2P: 3.15 (t, $^{2}J_{PH}$ = 9.9 Hz, 2H)[e] $N(CH_3)_2$: 2.75 (s/br, 24H)[e]	$N(CH_3)_2$: 49.8 (s/br)[e] PCH_2P: 24.1 (m/br)[e]
[Rh(COD)(*P*,*N*-Ph_2PAr)][OTf] (**9**)	38.3 (d, $^{1}J_{RhP}$ = 159 Hz, 1P)	NH: 7.08 (m/br, 1H), H_{COD}: 6.05 (m/br, 1H), 5.47 (m/br, 1H), 4.23 (m/br, 1H), 3.44 (m/br, 1H), 2.33 (br, 8H) NCH_3: 2.82 (d, $^{3}J_{HH}$ = 6.0, 3H)	NCH_3: 46.1 (s)

[a] NMR abbreviations: s = singlet, d = doublet, t = triplet, m = multiplet, br = broad. All NMR data recorded at 27 °C in CD_2Cl_2 unless otherwise indicated. [b] ^{31}P chemical shifts referenced to external 85% H_3PO_4. [c] ^{1}H and ^{13}C chemical shifts referenced to external tetramethylsilane. Chemical shifts for aryl groups not given. [d] NMR data recorded in C_6D_6. [e] C_2-symmetric isomer. [f] NMR data recorded in C_4D_8O. [g] C_s-symmetric isomer. [h] NMR data recorded at −80 °C.

dx.doi.org/10.1021/ic101883u |*Inorg. Chem.* 2011, 50, 5361–5378

(d) P,P′-1,2-bis(Diphenylphosphino)ethane(P,N-diphenyl(o-N-methylanilido)phosphine)rhodium(I), [Rh(P,P′-dppe)(P,N-Ph_2PAr^-)] (***3***). In a 50 mL Schlenk flask under anhydrous conditions and Ar atmosphere, dppe (71 mg, 178 μmol) and [Rh(COD)(*P*,*N*-Ph_2PAr^-)] (**1a**, 103 mg, 178 μmol) were dissolved in 7 mL of tetrahydrofuran at ambient temperature producing a red solution, which was stirred for 10 min. Stirring was stopped, the solution was carefully layered with 20 mL of *n*-pentane, and the mixture was left undisturbed for 18 h. The supernatant was removed by cannula transfer under Ar, then the solid was dried in vacuo and recovered as large red crystals (103 mg, 79% yield, found: C, 68.17; H, 5.70; N, 1.73%. Calcd for $[C_{45}H_{41}NP_3Rh]\cdot C_4H_8O$: C, 68.14; H, 5.72; N, 1.62%). Single crystals suitable for X-ray diffraction were obtained by slow evaporation from a tetrahydrofuran solution in an NMR tube.

(e) η^2-Peroxo(P,P′-1,2-bis(diphenylphosphino)ethane)(P,N-diphenyl-(o-N-methylanilido)phosphine)rhodium(III), [RhO_2(P,P′-dppe)(P,N-Ph_2PAr^-)] (***4***). In a 50 mL Schlenk flask under anhydrous conditions and Ar atmosphere, 10 mL of tetrahydrofuran was added to [Rh(*P*,*P*′-dppe)(*P*,*N*-Ph_2PAr^-)] (**3**, 31 mg, 36 μmol), and the mixture was stirred for 30 min resulting in a bright red solution. Oxygen was passed through the solution for 10 min with no noticeable color change, and 20 mL of *n*-pentane was then added resulting in an orange slurry, which was stirred for 30 min before allowing the precipitate to settle. The supernatant was removed by cannula transfer, and the red solid was then dried in vacuo (25 mg, 68% yield. HRMS (ESI): *m*/*z* 824.1473 $[M + H]^+$. Calcd for $C_{45}H_{42}NO_2P_3Rh$: 824.1478). Single crystals suitable for X-ray diffraction were obtained by slow evaporation from a benzene solution in an NMR tube.

(f) Iodo(methyl)(P,P′-1,2-bis(diphenylphosphino)ethane)(P,N-diphenyl(o-N-methylanilido)phosphine)rhodium(III), [RhI(CH_3)(P,P′-dppe)(P,N-Ph_2PAr^-)] (***5***). In a 50 mL Schlenk flask under anhydrous conditions and Ar atmosphere, [Rh(COD)(*P*,*N*-Ph_2PAr^-)] (**1a**, 157 mg, 271 μmol) and dppe (108 mg, 271 μmol) were dissolved in 10 mL of benzene at ambient temperature while stirring. Iodomethane (17 μL, 270 μmol) was then added via microsyringe resulting in an instantly noticeable darkening of the solution color. The solvent volume was reduced to approx 5 mL in vacuo, and 20 mL of diethyl ether was added while stirring to produce a red precipitate. The precipitate was allowed to settle from the mixture, and the supernatant was removed by cannula under Ar. The solid was dried in vacuo and isolated as a red powder (152 mg, 49% yield, found: C, 58.78; H, 5.13; N, 1.35%. Calcd for $[C_{46}H_{44}INP_3Rh]$: C, 59.18; H, 4.75; N, 1.50%). Although the crystal structure indicates 1 equiv of $C_4H_{10}O$ and 2 equiv of C_4H_8O per formula unit, a noncrystalline sample was analyzed here. ^{1}H NMR analysis in C_6D_6 (obtained at approximately the same time as the elemental analysis) was used to verify solvent content. Single crystals suitable for X-ray diffraction were obtained by layering a saturated tetrahydrofuran solution with diethyl ether in an NMR tube.

(g) P,P′-1,2-bis(Diphenylphosphino)ethane(P,N-diphenyl(o-N,N-dimethylanilinyl)phosphine)rhodium(I) Tetrafluoroborate, [Rh(P,P′-dppe)(P,N-Ph_2PAr')][BF_4] (***6***). In an NMR tube under Ar atmosphere, [Rh(*P*,*P*′-dppe)(*P*,*N*-Ph_2PAr^-)] (**3**, 21 mg, 24 μmol) and Me_3OBF_4 (4.0 mg, 27 μmol) were dissolved in 0.7 mL of CD_3NO_2 producing a dark yellow solution. $^{31}P\{^1H\}$ and ^{1}H NMR spectra reveal **6** as the major product along with [Rh(*P*,*P*′-dppe)(*P*,*N*-Ph_2PAr)][BF_4], suggesting the presence of moisture in the reaction mixture (generating HBF_4, which protonates at nitrogen). Despite our best efforts, we have not been able to isolate **6** as an analytically pure substance.

(h) η^2:η^2-1,4-Norbornadiene(P,N-diphenyl(o-N,N-dimethylanilinyl)-phosphine)rhodium(I) Tetrafluoroborate, [Rh(NBD)(P,N-Ph_2PAr')]-[BF_4] (***7a***). In a 50 mL Schlenk flask under anhydrous conditions and Ar atmosphere, Ph_2PAr' (94 mg, 308 μmol) and $[Rh(NBD)_2][BF_4]$ (115 mg, 308 μmol) were dissolved in 5 mL of dichloromethane at ambient temperature resulting in an orange solution, which was stirred for 5 min. Stirring was stopped, the solution was carefully layered with 10 mL of *n*-pentane, and the mixture was left undisturbed for 18 h. The supernatant was removed by cannula transfer under Ar; then the solid was dried in vacuo and recovered as large orange crystals (134 mg, 71% yield, found: C, 53.89; H, 4.89; N, 2.34%. Calcd for $[C_{27}H_{28}NPRh][BF_4]\cdot 0.25CH_2Cl_2$: C, 53.79; H, 4.72; N, 2.30%). ^{1}H NMR analysis in $CDCl_3$ (obtained at approximately the same time as the elemental analysis) was used to verify dichloromethane content. HRMS (ESI): *m*/*z* 500.1003 $[M]^+$. Calcd for $C_{27}H_{28}NPRh$: *m*/*z* 500.1009.

(i) η^2:η^2-1,4-Norbornadiene(P,N-di(o-N,N-dimethylanilinyl)phenylphosphine)rhodium(I) Tetrafluoroborate, [Rh(NBD)(P,N-$PhPAr'_2$)][BF_4] (***7b***). The compound was prepared in a manner similar to that of **7a** using $PhPAr'_2$ (153 mg, 439 μmol) and $[Rh(NBD)_2][BF_4]$ (164 mg, 439 μmol) and was isolated as a yellow-orange powder (231 mg, 83% yield, found: C, 55.42; H, 5.35; N, 4.37%. Calcd for $[C_{29}H_{33}N_2PRh][BF_4]$: C, 55.26; H, 5.28; N, 4.44%). HRMS (ESI): *m*/*z* 543.1425 $[M]^+$. Calcd for $C_{29}H_{33}N_2PRh$: *m*/*z* 543.1431.

(j) bis(η^2:η^2-1,4-Norbornadiene)(μ-P,N,P′,N′-bis(di(o-N,N-dimethylanilinyl)phosphino)methane)dirhodium(I,I) Bis(tetrafluoroborate), [Rh_2(NBD)$_2$(μ-P,N,P′,N′-dmapm)][BF_4]$_2$ (***8***). In a 50 mL Schlenk tube under anhydrous conditions and Ar atmosphere, dmapm (225 mg, 404 μmol) and $[Rh(NBD)_2][BF_4]$ (302 mg, 808 μmol) were dissolved in 10 mL of dichloromethane at ambient temperature resulting in an orange-red solution, which was then stirred for 5 min. To the stirred solution was added 20 mL of *n*-pentane resulting in the formation of a yellow precipitate. The slurry was stirred for 5 min before allowing the precipitate the settle. The supernatant was then removed by cannula transfer under Ar, and the product was isolated as a yellow powder (414 mg, 85% yield, found: C, 48.94; H, 5.10; N, 4.58%. Calcd for $[C_{47}H_{58}N_4P_2Rh_2][BF_4]_2\cdot 0.5CH_2Cl_2$: C, 49.06; H, 5.11; N, 4.82%). Although the crystal structure indicates 1 equiv of CH_2Cl_2 per formula unit, a noncrystalline sample was analyzed here, which was exposed to air before analysis. ^{1}H NMR analysis in $CDCl_3$ (obtained at approximately the same time as the elemental analysis) was used to verify dichloromethane content. Single crystals suitable for X-ray diffraction were obtained by layering a saturated dichloromethane solution with tetrahydrofuran in an NMR tube. HRMS (ESI): *m*/*z* 473.1117 $[M]^{2+}$. Calcd for $C_{47}H_{58}N_4P_2Rh_2$: *m*/*z* 473.1118.

(k) η^2:η^2-1,5-Cyclooctadiene(P,N-diphenyl(o-N-methylanilinyl)-phosphine)rhodium(I) Trifluoromethanesulfonate, [Rh(COD)(P,N-Ph_2PAr)][OTf] (***9***). In a 25 mL Schlenk tube under anhydrous conditions and Ar atmosphere, [Rh(COD)(*P*,*N*-Ph_2PAr^-)] (**1a**, 100 mg, 173 μmol) was dissolved in 2 mL of dichloromethane at ambient temperature producing an orange-red solution. While stirring, HOTf (16 μL, 180 μmol) was added, which turned the solution yellow after 5 min. To the stirred solution, 10 mL of *n*-pentane was added resulting in the formation of a yellow precipitate. Stirring was stopped, the precipitate was allowed to settle and the supernatant was removed by cannula transfer under Ar. The solid was then dried in vacuo and isolated as a yellow powder (76 mg, 63% yield, found: C, 49.36; H, 4.33; N, 2.14%. Calcd for $[C_{27}H_{30}NPRh][CF_3O_3S]\cdot 0.5CH_2Cl_2$: C, 49.33; H, 4.50; N, 2.02%). ^{1}H NMR analysis in $CDCl_3$ (obtained at approximately the same time as the elemental analysis) was used to verify dichloromethane content. Single crystals suitable for X-ray diffraction were obtained by slow evaporation from a dichloromethane solution in an NMR tube. HRMS (ESI): *m*/*z* 502.1170 $[M]^+$. Calcd for $C_{27}H_{30}NPRh$: 502.1165.

Low Temperature Protonation of [Rh(*P*,*P*′-dppe)(*P*,*N*-Ph_2PAr^-)] (3). In an NMR tube under anhydrous conditions and Ar atmosphere, **3** (25 mg, 29 μmol) was dissolved in 0.7 mL of CD_2Cl_2 at ambient temperature, and the bright red solution was immediately cooled to −80 °C in acetone/dry ice. Using a microsyringe, $HBF_4\cdot Et_2O$ (4.0 μL, 29 μmol) was added, resulting in a brilliant blue-green solution, and the temperature of the tube was maintained at −80 °C throughout the duration of subsequent ^{1}H, $^1H\{^{31}P\}$ and $^{31}P\{^1H\}$ NMR analyses (approximately 5 min).

dx.doi.org/10.1021/ic101883u |*Inorg. Chem.* 2011, 50, 5361–5378

General Protocol for Olefin Silylation Experiments. A representative procedure for the reaction of triethylsilane with styrene using [Rh(COD)(*P*,*N*-Ph_2PAr^-)] (**1a**) as the catalyst (Entry 3, Table 5) is as follows: In a 50 mL three-necked round-bottom flask equipped with a stir bar and attached reflux condenser, under anhydrous conditions and Ar atmosphere, **1a** (10.0 mg, 17.3 μmol) was dissolved in styrene (9.91 mL, 86.5 mmol), and the resulting red solution was heated to 60 °C for 10 min while stirring. Triethylsilane (2.76 mL, 17.3 mmol) was then added such that the molar ratio of Rh/$HSiEt_3$/styrene =1:1,000:5,000. The reaction temperature was maintained at 60 °C, and an overpressure of Ar was applied throughout the course of the reaction. The reaction mixture was sampled every 15 min for 3 h (relative to the addition of triethylsilane) by withdrawing a 0.5 mL aliquot from the reaction mixture and immediately adding it to 2.5 mL of dichloromethane containing 1.0 μL of HOTf. A 1.0 mL aliquot of this diluted solution was then quickly passed through a 4 cm Florisil column using an overpressure so that less than 30 s elapsed between removal of the sample from the reaction mixture and removal of the catalyst from the sample. The eluent was collected in a vial and stored at 0 °C in the dark until the reaction mixture could be analyzed by GC-MS and ^{1}H NMR spectroscopy. Reactions carried out in the presence of nitrobenzene were performed by first dissolving the catalysts in the appropriate volume of $C_6H_5NO_2$, followed by addition of the reagents as described above, so that the mole ratio of solution components was Rh/$HSiEt_3$/styrene/$C_6H_5NO_2$ = 1:1,000:5,000:1,000 in each case. Removal of cationic catalysts (**7a**, **7b**, and **8**) was easily accomplished (without HOTf) by passing reaction mixtures directly through a 4 cm Florisil column.

X-ray Structure Determinations. *(a) General Procedures.* Crystallographic experimental details for compounds **1a**, **2**, **3**, **4**, **5**, **8**, and **9** are provided in the Supporting Information section. Crystals were grown via slow diffusion of *n*-pentane into a benzene (**1a**) solution of the compound, diffusion of diethyl ether into a tetrahydrofuran (**5**) solution of the compound, diffusion of tetrahydrofuran into a dichloromethane (**8**) solution of the compound or by evaporation of a tetrahydrofuran (**2**, **3**), benzene (**4**), or dichloromethane (**9**) solution of the compound. Data were collected using Mo Kα radiation (λ = 0.71073 Å) on a Bruker APEX-II CCD detector/D8 diffractometer[40] with the crystals cooled to −100 °C. The data were corrected for absorption through use of a multiscan model (SADABS[40]) (**1a**, **2**) or through Gaussian integration from indexing of the crystal faces (**3**, **4**, **5**, **8**, **9**). Structures were solved using direct methods/structure expansion (SIR97[41]) (**1a**, **5**, **8**), direct methods (SHELXS-97[42]) (**2**, **4**, **9**), or Patterson search/structure expansion (DIRDIF-2008[43]) (**3**). Refinements were completed using the program SHELXL-97.[42] Hydrogen atoms were assigned positions based on the sp^2 or sp^3 hybridization geometries of their attached carbon or nitrogen atoms, and were given thermal parameters 20% greater than those of their parent atoms, except in the case of **2**, for which the positions of hydrogen atoms were refined.

(b) Special Refinement Conditions. Compound ***4***. One of the solvent benzene molecules was disordered over three sites; each was constrained as an idealized hexagon with C−C distances of 1.39 Å, and the carbon atoms were refined with occupancies of 1/3 and with a common isotropic displacement parameter.

RESULTS AND DISCUSSION

Phosphine-Amido Complexes. Reactions of [Rh(μ-OMe)(COD)]$_2$ with the protic monophosphinoaniline ligands, Ph_2PAr or $PhPAr_2$ (Ar = *o*-C_6H_4NHMe), in benzene at ambient temperature generate brilliant, red-orange solutions containing the neutral phosphine-amido complexes, [Rh(COD)(*P*,*N*-Ph_2PAr^-)] (**1a**, Ar^- = *o*-$C_6H_4NMe^-$) or [Rh(COD)(*P*,*N*-$PhP(Ar^-)Ar$)] (**1b**), resulting from *N*-deprotonation by the methoxide ion

Scheme 1. Synthesis of Phosphine-Amido Compounds 1a, 1b, and 2

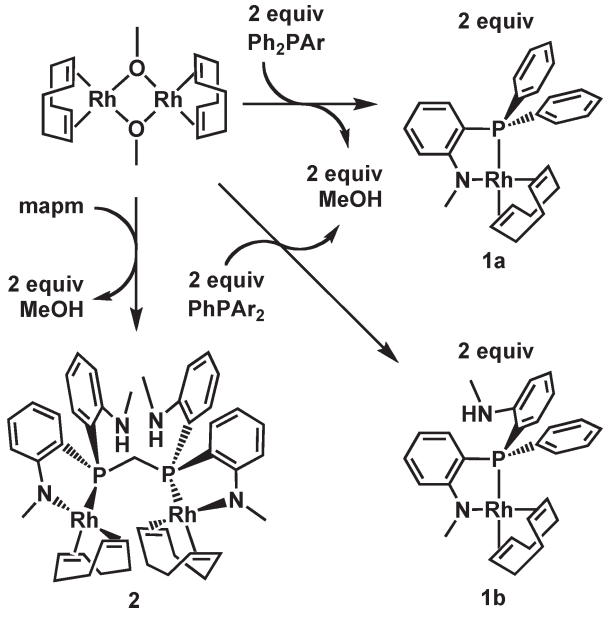

(Scheme 1). Replacement of a phenyl group in **1a** by an anilinyl group in **1b** creates a stereogenic center at phosphorus, and as a result, **1b** is chiral. The $^{31}P\{^1H\}$ NMR spectrum of **1a** displays the expected doublet at δ 41.2 with $^1J_{RhP}$ = 163 Hz, while the ^{1}H NMR spectrum shows a sharp singlet at δ 2.94 representing the *N*-methyl group, two distinct olefinic proton signals at δ 5.26 and 3.33, and the aliphatic ^{1}H resonances of the cyclooctadiene ligand as complex multiplets between δ 1.82 and 2.13. The $^{13}C\{^1H\}$ NMR spectrum shows the singlet *N*-methyl resonance at δ 39.1, which was identified by gradient heteronuclear multiple quantum coherence (gHMQC) analysis. For complex **1b**, the ^{31}P signal is shifted upfield (to δ 25.9) relative to that of **1a**, as is usually observed when the number of aniline groups is increased.[22] The ^{1}H NMR spectrum shows two sharp, distinct signals at δ 2.93 and 2.43 representing *N*-methyl groups belonging to the coordinated amido and pendent amine functionalities, respectively. Otherwise, the spectral parameters for both compounds are comparable.

The solid-state structure of **1a** (Figure 1) illustrates a square-planar ligand arrangement at rhodium in addition to a trigonal-planar geometry around the amido nitrogen atom; relevant bond lengths and angles are given in Table 2. The planarity of this amido group is demonstrated by the sum of the angles about nitrogen (359.9°), and the Rh−N distance (2.063(1) Å) is significantly shorter than the Rh−N single bond in the related phosphine-amine compound, [RhCl(CO)(*P*,*N*-Ph_2PAr)] (2.129(2) and 2.140(2) Å for the two independent molecules),[22] demonstrating a favorable π-interaction of the amido group with the metal. The C−C bond length of the alkene coordinated trans to the amido nitrogen (C(5)−C(6) = 1.405(2) Å) is significantly longer than that coordinated trans to the phosphine (C(1)−C(2) = 1.377(2) Å), while the Rh−C bond lengths opposite nitrogen are shorter (Rh−C(5) and Rh−C(6) = 2.140(1) and 2.137(1) Å, respectively) than those opposite phosphorus (Rh−C(1) and Rh−C(2) = 2.231(1) and 2.221(1) Å, respectively). While structural differences between the coordinated olefins perhaps reflect the π-donor character of the amido functionality, strengthening

dx.doi.org/10.1021/ic101883u |*Inorg. Chem.* 2011, 50, 5361–5378

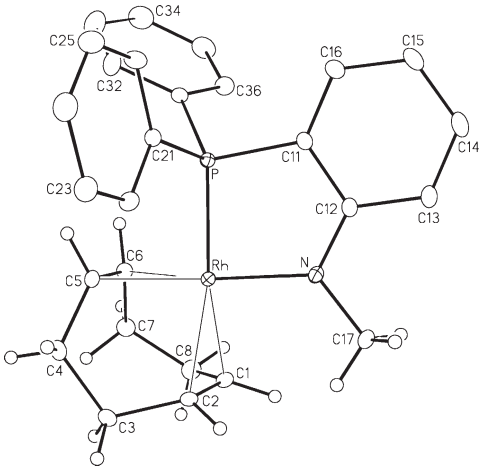

Figure 1. ORTEP Diagram of [Rh(COD)(*P*,*N*-Ph_2PAr^-)] (**1a**). Gaussian ellipsoids for all non-hydrogen atoms are depicted at the 20% probability level. Hydrogen atoms are shown with arbitrarily small thermal parameters for the cyclooctadiene and methyl groups, and are not shown for the aryl rings.

Table 2. Selected Structural Parameters for Compounds 1a and 2

atoms	**1a**·C_6H_6	**2**·C_4H_8O
	Bond Lengths (Å)	
Rh−P	2.2534(3)	2.261(1)
Rh−N(1)	2.063(1)	2.056(4)
C(1)−C(2)	1.377(2)	1.355(8)
C(5)−C(6)	1.405(2)	1.401(8)
P−C(11)	1.796(1)	1.819(4)
P−C(21)	1.823(1)	1.841(4)
P−C(31)	1.814(1)	
N(1)−C(12)	1.374(2)	1.340(6)
N(2)−C(22)		1.367(7)
C(11)−C(12)	1.423(2)	1.421(5)
C(12)−C(13)	1.424(2)	1.411(7)
C(13)−C(14)	1.385(2)	1.375(8)
C(14)−C(15)	1.393(2)	1.373(6)
C(15)−C(16)	1.386(2)	1.401(7)
C(16)−C(11)	1.392(2)	1.399(6)
Rh−C(1)	2.231(1)	2.204(5)
Rh−C(2)	2.221(1)	2.220(4)
Rh−C(5)	2.140(1)	2.136(5)
Rh−C(6)	2.137(1)	2.139(5)
	Angles (deg)	
P−Rh−N(1)	81.82(3)	81.3(1)
Rh−N(1)−C(17)	124.43(9)	123.3(3)
Rh−N(1)−C(12)	121.05(9)	123.1(3)
C(17)−N(1)−C(12)	114.4(1)	112.8(4)
P−C(10)−P′		122.8(3)
C(27)−N(2)−H(2N)		115(3)
C(22)−N(2)−H(2N)		113(3)
C(27)−N(2)−C(22)		121.3(5)

back-bonding to the olefin trans to it, the Rh−N−C(17) angle of 124.43(9)° is slightly expanded relative to that of a trigonal plane, suggesting that steric repulsion between the olefinic hydrogen atoms on C(1) and C(2) with the neighboring *N*-methyl group may also weaken the interaction of this olefin with rhodium. Indeed, the shortest H···H contact between these groups (2.12 Å) is slightly shorter than a normal van der Waals contact of 2.3 Å.[44]

A binuclear analogue of **1b** can be prepared much as reported above for the monophosphinoaniline complexes by using the previously reported mapm ligand ($Ar_2PCH_2PAr_2$).[22] Reaction of this protic diphosphinoaniline ligand with 1 equiv of [Rh-(μ-OMe)(COD)]$_2$ in tetrahydrofuran produces the binuclear species, [Rh_2(COD)$_2$(μ-*P*,*N*,*P*′,*N*′-$mapm^{2-}$)] (**2**, $mapm^{2-}$ = $Ar(Ar^-)PCH_2P(Ar^-)Ar$; Scheme 1), in which two of the four available amines are deprotonated to give amido functionalities at each metal, leaving two pendent amine groups. A $^{31}P\{^1H\}$ NMR spectrum shows a second order multiplet at δ 11.7 with $^1J_{RhP}$ = 165 Hz. The ^1H NMR spectrum shows a triplet resonance at δ 3.17 with $^2J_{PH}$ = 10.0 Hz corresponding to two chemically equivalent hydrogen atoms of the PCH_2P unit; the appearance of a single methylene resonance indicates that this species possesses C_2-symmetry (as depicted in Scheme 1) since for a C_s-symmetric complex with mutually *syn* coordination planes, these hydrogen atoms would be chemically distinct. When the above reaction was carried out in C_6D_6, an additional product in approx 15% yield was observed together with **2**. This minor, unidentified impurity displays a low intensity doublet in the $^{31}P\{^1H\}$ NMR spectrum at δ 15.1 with $^1J_{RhP}$ = 166 Hz, and may either be a C_s-symmetric isomer of **2** or a mononuclear tetradentate species with chemically equivalent phosphorus atoms. Whatever its identity, this impurity can be easily separated from **2** by precipitation of the latter with *n*-pentane and removal of the supernatant by cannula transfer.

We anticipated that coordination of a pendent amine at rhodium might produce a transient, 18-electron, five-coordinate intermediate, and that subsequent proton transfer from this amine to the adjacent amido nitrogen might invert one square plane with respect to the other. However, it appears that such amido/amine donor exchange does not occur at a spectroscopically observable rate, and there is no evidence to suggest that isomerization of the C_2-symmetric enantiomers, via a C_s-symmetric intermediate, is occurring in solution. The same is true for **1b**, the ^1H NMR spectrum of which shows sharp, well-resolved resonances for the *N*-methyl groups belonging to coordinated (amido) and pendent (amine) functionalities. Complexes **1a**, **1b**, and **2** are air-stable as solids, can be prepared in good yields, and are soluble in benzene, tetrahydrofuran, and dichloromethane.

A crystallographic analysis of **2** (Figure 2) illustrates the preferred *anti*-configuration of the rhodium coordination planes with respect to each other such that the molecule possesses C_2-symmetry in the solid state and crystallizes in a chiral space group (*C*2; see Supporting Information). Repulsion between the ligands on each metal and in particular, between the bulky COD ligands is minimized by a twisting of the diphosphine backbone about the P−CH_2 bonds, as seen in Figure 2 and further demonstrated by the Rh−P−P′−Rh′ torsion angle of 86.26(3)°, resulting in a 5.0994(6) Å separation of the metals. The large P−C(10)−P′ angle of 122.8(3)° is significantly expanded from the ideal tetrahedral arrangement at the methylene carbon, presumably a result of steric interactions between the COD group on one rhodium center with the anilido group on the other (see Figure 2). An analysis of the parameters in Table 2

dx.doi.org/10.1021/ic101883u |*Inorg. Chem.* 2011, 50, 5361–5378

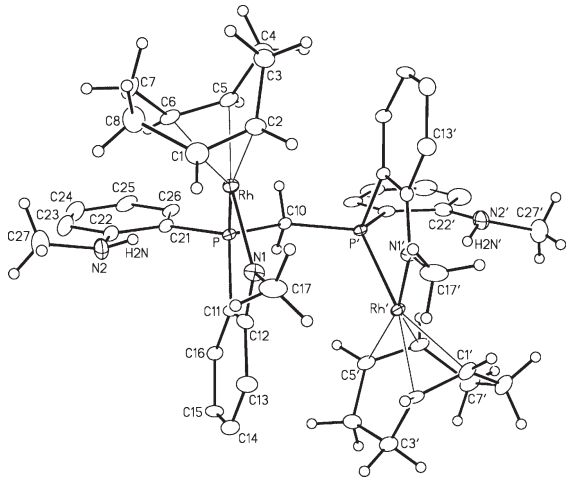

Figure 2. ORTEP Diagram of $[Rh_2(COD)_2(\mu\text{-}P,N,P',N'\text{-mapm}^{2-})]$ (**2**). Thermal ellipsoids as in Figure 1. Hydrogen atoms are shown with arbitrarily small thermal parameters for the cyclooctadiene, methyl, methylene, and amine groups, and are not shown for the aryl rings.

shows that the environment of each Rh center in **2** appears similar to that of **1a** as demonstrated by comparable bond lengths and angles in each complex; each half of **2** appears to be structurally similar to complex **1a**, with the obvious exception of the pendent amine groups in the former.

Inspection of the metrical parameters of the anilido groups in compounds **1a** and **2** reveals that the amido-aryl bonds (N−C(12) = 1.374(2) Å for **1a** and 1.340(6) Å for **2**) are significantly shorter than those within the previously reported phosphine-amine complex, $[RhCl(CO)(P,N\text{-}Ph_2PAr)]$ (1.468(3) and 1.465(4) Å for the two independent molecules),[22] while the arene C−C bonds involving the carbon atom *ipso* to an amido nitrogen, C(11)−C(12) and C(12)−C(13) within **1a** and **2** (ca. 1.42 Å), are significantly longer than all other C−C bonds within the amido-aryl groups (ca. 1.39 Å), or those of the adjacent phenyl groups (ca. 1.39 Å), as well as analogous bonds within the anilinyl ring of $[RhCl(CO)(P,N\text{-}Ph_2PAr)]$ (ca. 1.39 Å).[22] This pattern of bond lengths within the anilido groups is comparable to those of the previously reported ruthenium-amido complex, $[RuCl(\eta^6\text{-}p\text{-cymene})(P,N\text{-}Ph_2PAr^-)]$,[26] and suggests delocalization of the amido lone pair over the aromatic ring, as represented by the valence bond structures shown in Scheme 2. Such lone-pair delocalization has been suggested to result in the lower Brønsted basicity of aniline,[45] and it is anticipated that the electron withdrawing effect imposed by the aryl substituent at nitrogen within these amido complexes will play a role in their reactivity.

Interestingly, refinement of the amine hydrogen (H2N) on the pendent anilinyl group in **2** reveals somewhat alleviated pyramidalization of N(2), as made evident by the sum of the angles at this atom (349°), which is intermediate between those of idealized planar (360°) and pyramidal (328°) geometries. The effect is also observed within pendent *N,N*-dimethylanilinyl groups of related species, for which the sum of the angles at the trivalent nitrogen atom is typically near 336°.[22,26] Although the uncertainty in X-ray-determined hydrogen positions makes it difficult to determine the degree of planarity or pyramidalization of N(2), the pattern of bond lengths within the rest of the anilinyl group (see Supporting Information), which closely mirrors that displayed by the anilido groups in this compound and in compound **1b**, argues strongly in favor of a more planar geometry

Scheme 2. Possible Resonance Description of Compound 1a

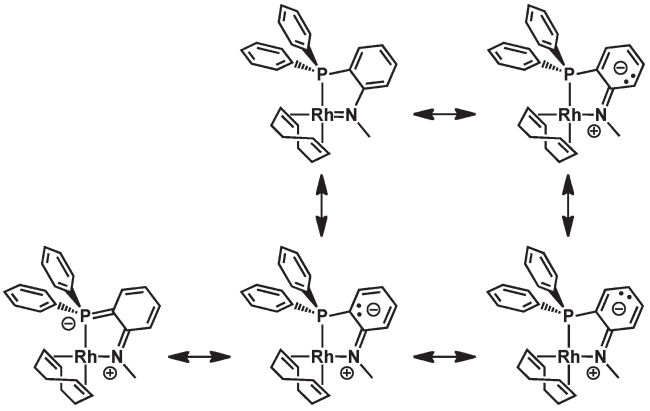

in which the amine lone pair is delocalized over the aryl ring. Also evident in the structures of compounds **1a** and **2** are the somewhat shorter P−C bond lengths involving the anilido substituent (**1a**: 1.796(1) Å; **2**: 1.817(5) Å) compared to those involving the other aryl groups (**1a**: 1.823(1), 1.814(1) Å; **2**: 1.840(4) Å), supporting the contribution of the resonance structure shown at the bottom-left of Scheme 2, although these differences appear less dramatic than those involving the N−C bonds.

Although **1a** may appear similar in many respects to Grützmacher's ketone hydrogenation catalyst, $[Rh(P(Tol)Ph_2)(\eta^2\text{:}\eta^2\text{-}N\text{-(dibenzotropylidenyl)}_2N^-)]$ (which rapidly reacts with molecular hydrogen to form an amine hydride),[8] reactions of either **1a** or **2** with hydrogen at ambient pressure and temperature in tetrahydrofuran solutions result in decomposition, presumably by hydrogenation of the diolefin. In an attempt to produce a species that would react cleanly with molecular hydrogen to produce a stable complex, the cyclooctadiene ligand of **1a** was replaced by a chelating diphosphine. The reaction of **1a** with 1 equiv of 1,2-bis(diphenylphosphino)ethane (dppe) in tetrahydrofuran under inert conditions results in the facile generation of $[Rh(P,P'\text{-dppe})(P,N\text{-}Ph_2PAr^-)]$ (**3**, Scheme 3), which can be isolated as large, red crystals in good yield.

The $^{31}P\{^1H\}$ NMR spectrum of **3** (Figure 3) shows the expected signal pattern for an ABCX spin-system with a downfield resonance at δ 67.9 corresponding to the phosphine unit trans to the amido donor. The resonances of the mutually trans phosphine donors appear at δ 59.0 and 46.0 and are identified by their strong mutual coupling ($^2J_{PP}$ = 311 Hz). The ^1H NMR spectrum of **3** shows a singlet *N*-methyl signal at δ 2.93 and complex multiplets for the dppe methylene protons centered around δ 2.00. The aliphatic ^{13}C resonance, found at δ 47.0, was identified as belonging to the *N*-methyl group by gHMQC analysis via correlation to the attached protons, while the signals at δ 30.2 and 26.3 correlate to the dppe methylene protons.

The X-ray structure of compound **3** (Figure 4) depicts the square-planar complex with a somewhat shortened Rh−P(3) bond of only 2.2120(4) Å for the end of the diphosphine donor trans to the amido functionality, and relatively long Rh−P(1) and Rh−P(2) bonds for the mutually trans phosphines at 2.2939(4) and 2.2737(4) Å, respectively (Table 3), consistent with the greater trans-influence of the phosphine groups. An interesting structural feature of this complex involves the close-to-parallel arrangement of the phenyl groups on P(1) and P(3)

dx.doi.org/10.1021/ic101883u |*Inorg. Chem.* 2011, 50, 5361–5378

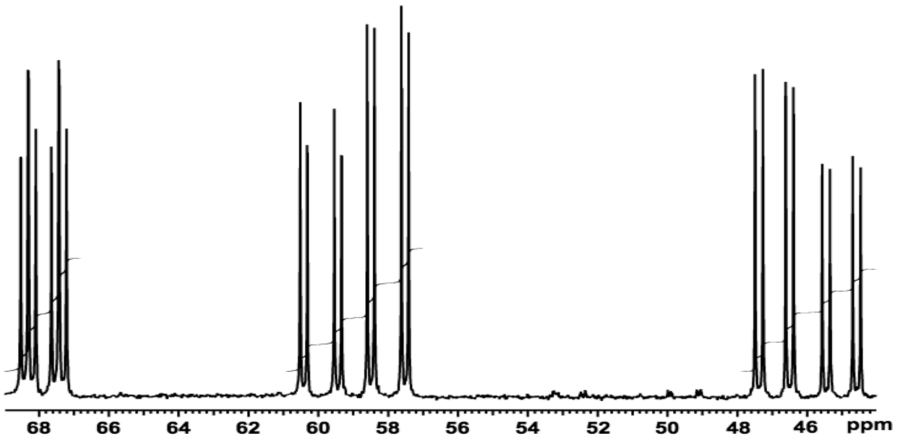

Figure 3. $^{31}P\{^{1}H\}$ NMR Spectrum of [Rh(*P*,*P*′-dppe)(*P*,*N*-Ph_2PAr^-)] (**3**).

Scheme 3. Synthesis of Phosphine-Amido Compounds 3− 6

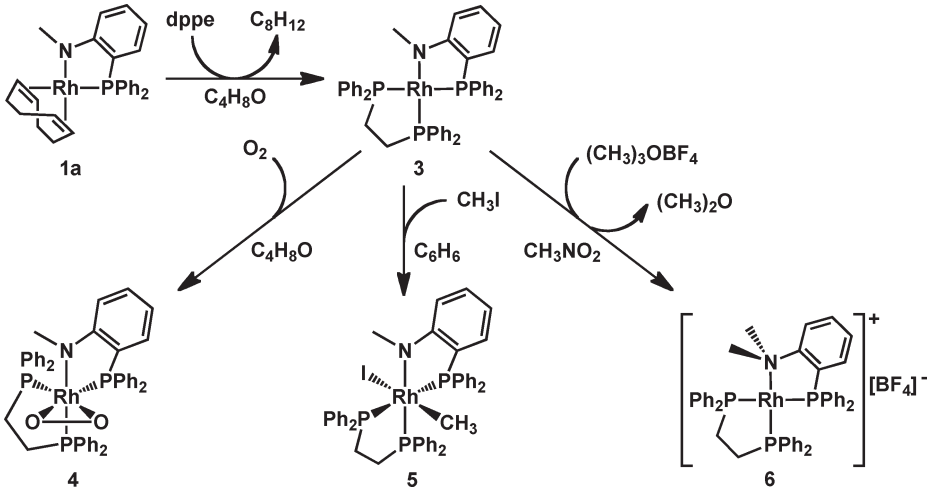

on the same side of the rhodium coordination plane. Despite the proximity of the carbon atoms on adjacent phenyl groups (i.e., C(66)···C(32) = 3.35 Å), which are comparable to those between layers of graphite,[47] the expanded P(1)−Rh−P(3) angle of 97.28(1) ° suggests that the parallel arrangement of these groups simply minimizes steric contacts and is not the result of attractive $\pi-\pi$ interactions. The Rh−N distance in **3** (2.085(1) Å) is slightly elongated relative to those of **1a** (2.063(1) Å) and **2** (2.056(4) Å) perhaps illustrating decreased π-donor character of the amido group because of the absence of the trans olefin π-acceptor. Again, the short N−C(12) distance (1.359(2) Å) is indicative of partial double bond character and delocalization of the lone pair over the aryl group, which is also made evident by the pattern of C−C bond lengths within the anilido ring (see Supporting Information), as noted above for compounds **1a** and **2**.

Surprisingly, compound **3** in tetrahydrofuran at ambient temperature is inert to dihydrogen as judged by NMR analysis, even after a 24 h exposure. It appears that the amido group is neither nucleophilic enough to deprotonate hydrogen, nor a strong enough donor to promote H_2 oxidative addition at rhodium under ambient conditions. The delocalization of the nitrogen lone pair over the aryl ring, as noted above, is undoubtedly playing a role in modulating the basicity of the amido group. A structurally related complex, [$Rh(PPh_3)_2$(*P*,*N*-$Ph_2PC_6H_4$-NH^-)], has also been prepared, and although it was found to be inactive as a ketone hydrogenation catalyst, its direct reaction with hydrogen was not reported.[46] Although unreactive toward H_2, compound **3** does display the ability to undergo oxidative addition in two other cases examined. Compound **3** is stable in air for days as a crystalline solid, but solutions of this complex react immediately with molecular oxygen upon exposure to air (unlike **1a**, **1b**, or **2**) to afford the peroxo derivative, [RhO_2(*P*,*P*′-dppe)(*P*,*N*-Ph_2PAr^-)] (**4**, Scheme 3). This sparingly soluble compound can be dissolved in CD_2Cl_2 to allow NMR characterization; however, slow decomposition is observed in this solvent. The $^{31}P\{^{1}H\}$ NMR spectrum of **4** shows three ddd signals at δ 52.7, 50.1, and 38.7 with the largest $^{2}J_{PP}$ coupling constant of only 20 Hz, indicating the absence of mutually trans phosphines in this complex. In contrast to compound **3**, a ^{1}H NMR analysis of **4** shows splitting of the *N*-methyl resonance into a doublet with $^{4}J_{PH}$ = 4.4 Hz and the coupling interaction (most likely due to the trans phosphine) was verified by $^{1}H\{^{31}P\}$ NMR analysis, showing collapse of the doublet resonance to a singlet.

dx.doi.org/10.1021/ic101883u |*Inorg. Chem.* 2011, 50, 5361–5378

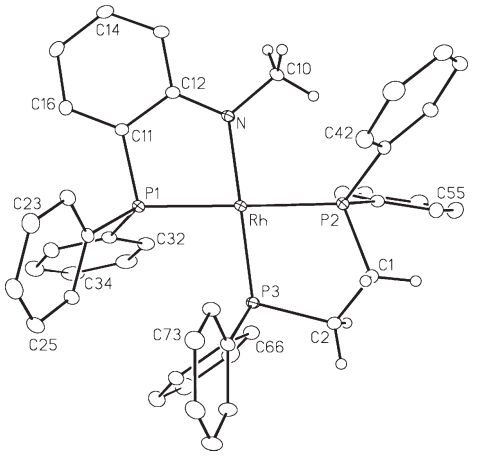

Figure 4. ORTEP Diagram of [Rh(*P*,*P*′-dppe)(*P*,*N*-Ph_2PAr^-)] (**3**). Thermal ellipsoids as in Figure 1. Hydrogen atoms are shown with arbitrarily small thermal parameters on methyl and methylene groups, and are not shown for the aryl rings.

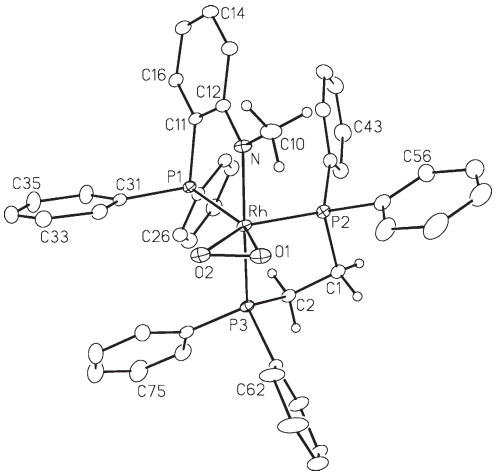

Figure 5. ORTEP Diagram of [RhO_2(*P*,*P*′-dppe)(*P*,*N*-Ph_2PAr^-)] (**4**). Thermal ellipsoids as in Figure 1. Hydrogen atoms are shown with arbitrarily small thermal parameters on methyl and methylene groups, and are not shown for the aryl rings.

Table 3. Selected Structural Parameters for Compounds 3−5

atoms	**3**·C_4H_8O	**4**·2.5C_6H_6	**5**·$C_4H_{10}O$·2C_4H_8O
		Bond Lengths (Å)	
Rh−P(1)	2.2939(4)	2.3096(7)	2.3228(6)
Rh−P(2)	2.2737(4)	2.3009(8)	2.4006(6)
Rh−P(3)	2.2120(4)	2.2914(7)	2.3183(6)
Rh−N	2.085(1)	2.098(2)	2.117(2)
Rh−O(1), Rh−O(2)		2.024(2), 2.054(2)	
O(1)−O(2)		1.440(3)	
Rh−I			2.8028(3)
Rh−C(1)			2.098(2)
N−C(12)	1.359(2)	1.350(4)	1.347(3)
		Angles (deg)	
P(1)−Rh−P(2)	178.50(1)	100.00(3)	173.72(2)
P(3)−Rh−N	178.04(4)	176.99(7)	178.65(6)
P(1)−Rh−N	81.98(4)	81.44(7)	80.07(6)
P(2)−Rh−P(3)	83.73(1)	84.96(3)	84.27(2)
P(1)−Rh−P(3)	97.28(1)	96.88(3)	100.66(2)
I−Rh−C(1)			176.16(7)

A crystallographic analysis of **4** shows a pseudotrigonal bipyramidal geometry at rhodium (Figure 5) in which the axial sites are occupied by one end of the dppe group and the amido donor, while the other end of the dppe group, the O_2 moiety and the *P*-terminus of the phosphine-amido group occupy the equatorial positions. A structural comparison of **3** and **4** demonstrates that O_2 binding to **3** retains the mutually trans arrangement of the amido group and one end of the dppe ligand, with the other ends of both chelates bending back to accommodate O_2. Table 3 shows that the O−O bond length (1.440(3) Å) is comparable to that found in the O_2 adduct of Vaska's complex (1.47(1) Å),[48] in which O_2 is reversibly bound.[49] However, **4** shows no evidence of O_2 loss after being subjected to an Ar purge for 10 min or to vacuum for 1.5 h as made evident by the unchanged $^{31}P\{^1H\}$ NMR spectrum. The P(1)−Rh−P(2) angle of 100.00(3)° is intermediate between the angles expected for octahedral and trigonal bipyramidal geometries; the former geometric description is appropriate when considering the complex as a Rh(III)-peroxide, and the latter as a Rh(I)-dioxygen adduct. A comparison of structures **3** and **4** illustrates elongation of the mutually trans Rh−P(3) and Rh−N bonds in the latter—a feature that is particularly interesting considering that the spectroscopically observed $^4J_{PH}$ in compound **4** (vide supra) is not seen in the ^1H NMR spectrum of compound **3**. As expected, all Rh−L distances in **4** are longer than those in **3** owing to increased steric crowding caused by coordination of the O_2 ligand.

Compound **3** bears some resemblance to a phosphine-amido complex prepared by Fryzuk et al., which was shown to undergo oxidative additions of halomethanes.[50] We thought that **3** might react with iodomethane in an analogous manner, but were also curious about the possibility that subsequent methyl migration to the amido group could occur to generate a complex with a labile *N*,*N*-dimethylanilinyl substituent. We find that addition of iodomethane to 1 equiv of **3** in benzene results in an immediate darkening of the initially red solution, signaling the formation of the oxidative addition product, [RhI(CH_3)(*P*,*P*′-dppe)(*P*,*N*-Ph_2PAr^-)] (**5**, Scheme 3). The pattern observed in the $^{31}P\{^1H\}$ NMR spectrum, is typical of an ABCX spin system and demonstrates a large coupling constant ($^2J_{PP}$ = 445 Hz) between a pair of ^{31}P nuclei indicating that a mutually trans arrangement of phosphine donors has been maintained in the product. The ^1H NMR spectrum reveals a singlet resonance at δ 3.41 corresponding to one *N*-methyl group, as well as four distinct multiplets between δ 3.60 and 2.02, each representing one of the chemically unique methylene protons of the dppe ligand. An upfield doublet at δ 0.79 ($^2J_{RhH}$ = 2.0 Hz), integrating as three protons, represents the rhodium-bound methyl group. Compound **5** is remarkably stable in refluxing benzene and methyl migration to the amido group to produce [Rh(*P*,*P*′-dppe)(*P*,*N*-Ph_2PAr')]I or [RhI(*P*,*P*′-dppe)(*P*-Ph_2PAr')] is never observed.

A crystallographic study of **5** was carried out to unambiguously establish the geometry (cis or trans arrangement of CH_3 and I ligands) and to compare structural characteristics with those of its square planar precursor (**3**) and pseudotrigonal bipyramidal peroxo complex (**4**). The X-ray structure of **5** (Figure 6) shows

dx.doi.org/10.1021/ic101883u |*Inorg. Chem.* 2011, 50, 5361–5378

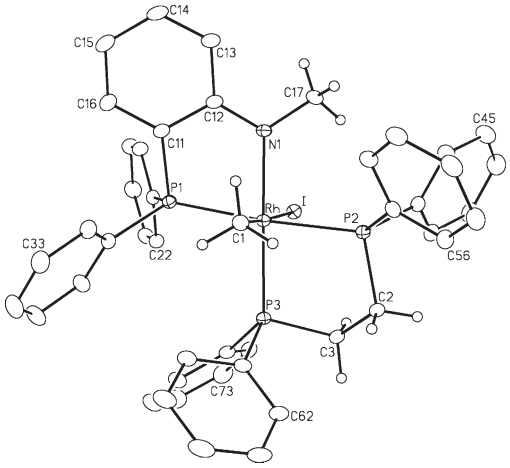

Figure 6. ORTEP Diagram of [RhI(CH_3)(*P*,*P*′-dppe)(*P*,*N*-Ph_2PAr^-)] (**5**). Thermal ellipsoids as in Figure 1. Hydrogen atoms are shown with arbitrarily small thermal parameters on methyl and methylene groups, and are not shown for the aryl rings.

the anticipated octahedral geometry at rhodium having the iodo and methyl groups in a mutually trans arrangement (as is often observed),[51] and is consistent with nucleophilic displacement of I^- from CH_3I by the Rh complex (**3**). The structure of **5** reveals an expanded square plane of pnictogen donor atoms relative to **3**, made evident by a comparison of bond lengths at rhodium within these two species (Table 3), presumably a result of steric crowding in this 6-coordinate complex, bearing the large iodo ligand. With the exception of a slight deviation of the P(1)−Rh−P(2) angle from linearity in **5**, other angles at rhodium are similar to those of complex **3**. As was described above for compounds **1a** and **2**, the N−C(12) bond lengths in each of the phosphine-amido compounds **3**, **4**, and **5** (1.359(2), 1.350(4) and 1.347(3) Å, respectively) are also significantly contracted relative to those of the previously reported phosphine-amine compound, [RhCl(CO)(*P*,*N*-Ph_2PAr)] (1.468(3) and 1.465(4) Å for the two independent molecules),[22] and these compounds also display an almost identical pattern of bond lengths within the anilido rings (see Supporting Information), suggesting significant delocalization of the amido lone pair over the aromatic ring in each case.

The propensity for oxidative addition of iodomethane to **3**, rather than its heterolysis by the amido-rhodium functionality, reflects an electron-rich rhodium atom and a relatively inert amido group, consistent with the crystallographically inferred delocalization of electron density over both the metal and the aromatic system. However, the well established existence of *P*,*N*-coordinated *N*,*N*-dimethylanilinylphosphines,[22,26] including our synthesis of [Rh(*P*,*P*′-dppe)(*P*,*N*-Ph_2PAr')][BF_4] (**6**, Ar′ = *o*-$C_6H_4NMe_2$), generated by sequential reactions of Ph_2PAr' and dppe ligands with [$Rh(NBD)_2$][BF_4] (discussed later), suggests that alkylation of the amido nitrogen in **3**, to give an *N*,*N*-dimethylanilinyl group should be possible, perhaps by using a harder methyl cation. Indeed, the addition of trimethyloxonium tetrafluoroborate (Me_3OBF_4) to **3** in nitromethane produces [Rh(*P*,*P*′-dppe)(*P*,*N*-Ph_2PAr')][BF_4] (**6**, Scheme 3). Compound **6** appears as three ddd signals in the $^{31}P\{^1H\}$ spectrum at δ 69.2, 55.0, and 43.1, and the ^1H NMR spectrum shows a singlet at δ 3.03 representing the two chemically equivalent *N*-methyl groups, consistent with the representation provided in Scheme 3. In principle, this complex could undergo isomerization to an analogue of **5** by an oxidative 1,2-methyl migration from N to Rh. However, the absence of an upfield Rh-methyl resonance in the ^1H NMR spectrum shows that such a process has not occurred, presumably because of the poor coordinating ability of the tetrafluoroborate counterion, which cannot provide electronic saturation that would favor a rhodium(III) species. Even the addition of KI to **6** in CD_3NO_2 did not result in its conversion to **5**. We thought that perhaps the opposite might also be possible, in which the iodo/methyl complex **5** could be converted into **6** by reductive elimination of methyl and amido groups. However, attempts to produce **6** by iodide abstraction from **5** with $AgBF_4$ in dichloromethane, nitromethane, or benzene under anhydrous, inert conditions in the dark consistently resulted in complex intractable mixtures. The alternate use of thallium salts for chloride-ion abstraction was not attempted.

Having observed alkyl group addition at either rhodium or the amido nitrogen, we sought to determine the possible site(s) of protonation in **3**. The reaction of **3** with 1 equiv of $HBF_4 \cdot Et_2O$ in CD_2Cl_2 at ambient temperature initially produces a blue-green solution that turns yellow within a few seconds. The yellow solution can be shown to contain [Rh(*P*,*P*′-dppe)(*P*,*N*-Ph_2PAr)][BF_4], in which the proton is *N*-bound, as made evident by a doublet resonance in the ^1H NMR spectrum, representing the *N*-methyl group at δ 2.39 (with $^3J_{HH}$ = 4.8 Hz), a broad quartet for the amine hydrogen at δ 8.21, and no hydride signal. We thought that the initially observed blue-green color might represent protonation at rhodium to generate a hydrido intermediate, from which 1,2-proton migration to nitrogen generates the thermodynamic product. However, when the reaction is repeated at −80 °C, low temperature NMR analysis of the blue-green solution reveals two kinetic intermediates in the $^{31}P\{^1H\}$ spectrum in an approximate 1:1 ratio, each with an ABCX signal pattern. Interestingly, the ^1H and $^1H\{^{31}P\}$ NMR spectra show no evidence of a hydride signal from δ 1.5 through −20.0. However, numerous, unprecedented multiplets appearing between δ 4.5 to 6.5 suggest that protonation occurs kinetically at the *ortho* or *para* positions of the anilinyl ring to produce cationic phosphine-imine intermediates that isomerize to the thermodynamic product via imine-enamine tautomerization, as shown for protonation at one of the *ortho* positions in Scheme 4. The absence of a hydride resonance in the upfield region and the presence of several new signals in the downfield region of the ^1H spectrum at −80 °C seem to indicate that the arene is the most nucleophilic site in **3**. Warming to ambient temperature then quickly produces a yellow solution, accompanied by disappearance of many of the signals between δ 4.5−6.5 to give [Rh(*P*,*P*′-dppe)(*P*,*N*-Ph_2PAr)][BF_4]. Protonation at either the *ortho* or *para* positions of the aryl group is consistent with the crystallographically inferred delocalization of the amido lone pair over the aromatic ring (see Scheme 2), as are the dramatic color changes observed as aromaticity is broken (upon protonation at carbon) and subsequently regenerated (upon proton migration to nitrogen). Reversible dearomatization has also been shown to occur within Milstein's dehydrogenation catalyst, which employs a pyridine-based *P*,*N*,*N*-ligand.[52]

In attempts to confirm the proposed kinetically preferred site of protonation of **3** at the aryl ring we considered the use of deutero-acids that should result in deuterium incorporation into the *ortho* and *para* positions of the ring. We did not investigate the use of DOTf, since previous attempts to protonate **3** with HOTf had resulted in mixtures of products over a wide temperature range. Furthermore, since $DBF_4 \cdot Et_2O$ was not readily

dx.doi.org/10.1021/ic101883u |*Inorg. Chem.* 2011, 50, 5361–5378

Scheme 4. Protonation of 3 via a Possible Phosphine-Imine Intermediate

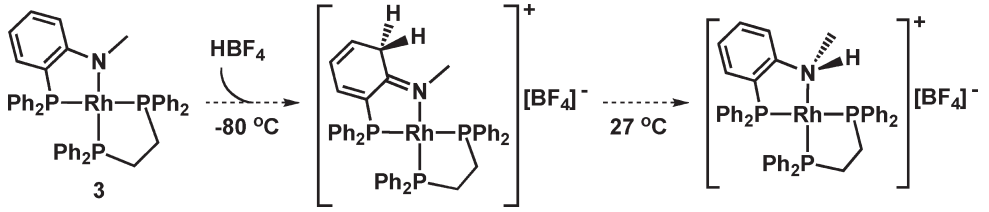

available, we instead investigated the reaction of **3** with $[D(OEt_2)_2][BAr^F{}_4]$ (Ar^F = 3,5-$(CF_3)_2C_6H_3$).[53] Surprisingly, the reaction with $[D(OEt_2)_2][BAr^F{}_4]$ proceeded differently than with $HBF_4 \cdot Et_2O$ and no blue-green color was observed over the temperature range from −80 °C to ambient. In this case, the only product observed is the amine, $[Rh(P,P'\text{-dppe})(P,N\text{-}Ph_2PAr)][BAr^F{}_4]$, resulting from exclusive deuteration at the amido nitrogen of **3**.

Phosphine-Amine Complexes. *(a) Generation from Phosphine-Amines.* Hemilabile complexes are readily formed by the displacement of a norbornadiene group in $[Rh(NBD)_2]^+$ by a phosphine-amine ligand. Reactions of $[Rh(NBD)_2][BF_4]$ with 1 equiv of Ph_2PAr' or $PhPAr'_2$ (Ar' = o-$C_6H_4NMe_2$) in dichloromethane result in the formation of phosphine-amine products, $[Rh(NBD)(P,N\text{-}Ph_2PAr')][BF_4]$ (**7a**) or $[Rh(NBD)(P,N\text{-}PhPAr'_2)][BF_4]$ (**7b**, Scheme 5), respectively. Compound **7a** shows the expected doublet in the $^{31}P\{^1H\}$ NMR spectrum at δ 37.7, while its ambient temperature ^1H NMR spectrum shows three broad signals at δ 5.62, 4.12, and 1.72, in a 1:2:1 intensity ratio, representing the norbornadiene methine, olefin, and methylene hydrogen atoms, respectively. The observation of only three ^1H signals for the norbornadiene group (rather than five signals in a 2:2:2:1:1 ratio, expected for the static geometry shown in Scheme 5) suggests chemical exchange via a fluxional process in which the olefinic groups opposite P and N are exchanging. At −80 °C, the spectrum shows two partially resolved olefinic proton resonances as well as two distinct doublets representing the methylene protons. At −60 °C, coalescence of the olefinic proton signals is observed with an exchange rate constant of k_{coal} = 18 s^{-1} corresponding to an activation barrier of $\Delta G^{\ddagger}$ (213 K) = 11 kcal/mol. This chemical exchange can be rationalized either by a process involving Rh−N bond rupture trans to one olefin, via a transient 14 e^- intermediate, rotation about the Rh−P bond, followed by reformation of the Rh−N bond cis to this olefin, or by lability of the norbornadiene ligand. To test whether lability of the norbornadiene or Ph_2PAr' ligands accounts for the observed fluxionality, **7a** was reacted with 1 equiv of dppe in CD_2Cl_2. The resulting $^{31}P\{^1H\}$ NMR spectrum shows a 1:1:1 mixture of $[Rh(NBD)(P,P'\text{-dppe})][BF_4]$ (δ 57.0, $^1J_{RhP}$ = 153 Hz),[54] $[Rh(P,P'\text{-dppe})(P,N\text{-}Ph_2PAr')][BF_4]$ (**6**), and free Ph_2PAr' (δ −12.2) suggesting that both the norbornadiene and Ph_2PAr' ligands are susceptible to displacement by the chelating diphosphine. Compound **6** displays a signal pattern characteristic of an ABCX spin system in the $^{31}P\{^1H\}$ NMR spectrum similar to that of **3**, inspiring its preparation by addition of Me_3OBF_4 to **3** (vide supra).

The displacement of both phosphine-amine and norbornadiene ligands by dppe suggests that their labilities are comparable, and that the observation of chemical exchange may be the result of more than one fluxional process. Although hemilability of the related $PhPAr'_2$ and PAr'_3 ligands at rhodium has already been found to occur by rapid and reversible displacement of the coordinated amine by a pendent one,[22] in this case, hemilability of the Ph_2PAr' ligand implies the involvement of a coordinatively unsaturated species, which may allow for more facile substrate coordination/activation in catalysis. The $^{31}P\{^1H\}$ NMR spectrum of **7b** shows a signal at δ 27.5, shifted upfield relative to that of **7a**. Like that of **7a**, the ambient temperature ^1H NMR spectrum of **7b** also shows three broad resonances representing the norbornadiene group, as well as a single resonance at δ 2.84 representing all four rapidly exchanging *N*-methyl groups. The observation of only one *N*-methyl signal indicates exchange of the amines at rhodium by a Type II[2] hemilabile process similar to those occurring within the previously reported species, $[RhCl(CO)(P,N\text{-}PhPAr'_2)]$ and $[RhCl(CO)(P,N\text{-}PhPAr_2)]$.[22]

Scheme 5. Synthesis of Phosphine-Amine Compounds 7a, 7b, and 8

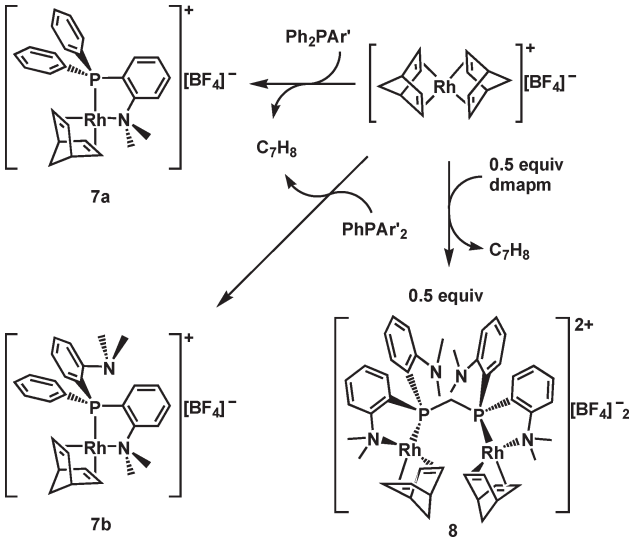

Reaction of the diphosphinoaniline, dmapm ($Ar'_2PCH_2PAr'_2$), with 2 equiv of $[Rh(NBD)_2][BF_4]$ in dichloromethane results in the generation of the binuclear analogue of **7b**, namely, $[Rh_2(NBD)_2(\mu\text{-}P,N,P',N'\text{-dmapm})][BF_4]_2$ (**8**, Scheme 5), which like compound **2**, places the rhodium coordination planes *anti* to each other so that the dication is C_2-symmetric. The ambient temperature $^{31}P\{^1H\}$ NMR spectrum of this compound shows a broadened second order multiplet at δ 12.0 with $^1J_{RhP}$ = 180 Hz (Figure 7). Upon cooling, however, the signal shows further broadening, followed by decoalescence (at approx −60 °C), finally producing a less intense multiplet at δ 7.4 in addition to a more intense multiplet at δ 9.7 (at −80 °C). We propose that the less intense, more upfield signal results from

dx.doi.org/10.1021/ic101883u |*Inorg. Chem.* 2011, 50, 5361–5378

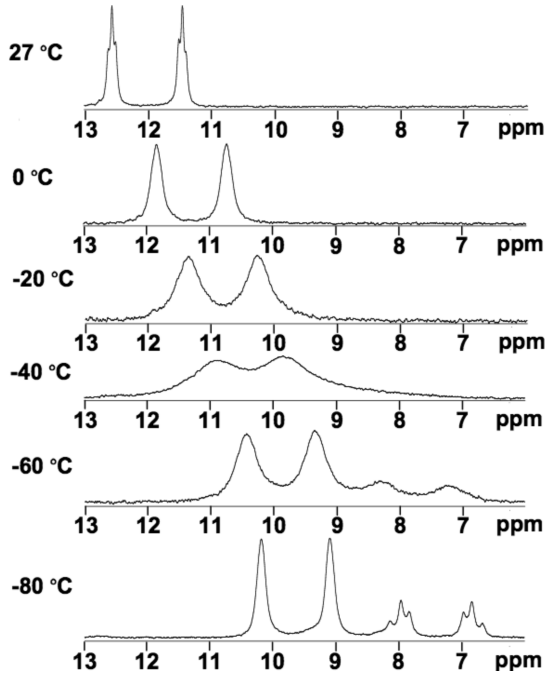

Figure 7. $^{31}P\{^{1}H\}$ NMR Spectra of Compound **8** (in 6:1 (v/v) CD_2Cl_2/CD_3NO_2).

the C_s-symmetric isomer of **8**, having mutually *syn* coordination planes, acting as an intermediate through which interconversion of C_2-symmetric enantiomers occurs. Such a transformation, which may involve sequential displacement of each coordinated amine by the adjacent, pendent one was observed for a similar complex, although in this case the speculated C_s-symmetric intermediate could not be directly observed.[22] It is not clear why the ^{31}P chemical shifts for **8** display the temperature dependence observed. An ambient temperature, ^{1}H NMR analysis of **8** shows a triplet at δ 3.15 representing the chemically equivalent PCH_2P hydrogens of the C_2-symmetric species as well as a single broad resonance at δ 2.75 representing all *N*-methyl protons. Unfortunately, all ^{1}H signals broaden dramatically and irregularly upon cooling to −80 °C, precluding low temperature characterization.

The solid state structure of **8** (dication shown in Figure 8) has the expected *anti* arrangement of the coordination planes as was observed for **2** (vide supra) and all other structural parameters appear normal with the exception of the expanded P(1)−C(10)−P(2) angle of 123.0(1)° (Table 4), which appears to be due to transannular steric relief, much as observed for **2**. As was also observed for **2**, the staggering of the Rh positions about the bridging diphosphine backbone is seen in the Rh(1)−P(1)−P(2)−Rh(2) torsion angle of 57.29(2)°. The nitrogen atoms within the pendent *N*,*N*-dimethylaniline groups of **8** are pyramidalized, as made evident by the sums of the angles at N(2) and N(4) (ca. 333°), contrasting the relatively planar geometry observed for the pendent *N*-methylaniline group in **2** (sum of angles at N(2) = 349°). The greater pyramidalization at nitrogen upon substitution of a hydrogen atom by a methyl group may reflect the more electropositive nature of H[55,56] favoring sp^2 over sp^3 hybridization, as rationalized by Bent's rule.[57]

(b) Generation from Phosphine-Amido Complexes. The reactivity of phosphine-amido complexes discussed earlier has

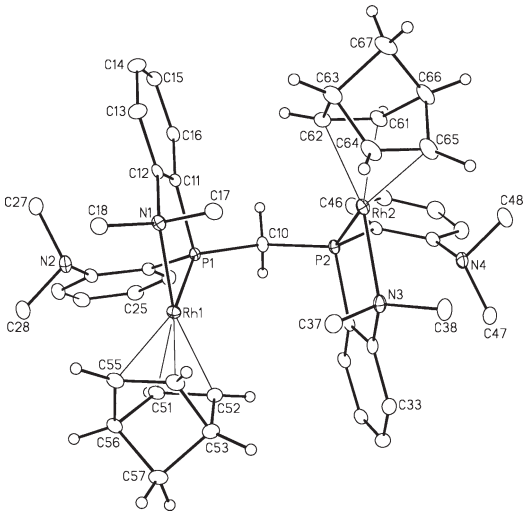

Figure 8. ORTEP Diagram of the dication of $[Rh_2(NBD)_2(P,N,P',N'\text{-dmapm})][BF_4]_2$ (**8**). Non-hydrogen atoms are represented by Gaussian ellipsoids at the 20% probability level. Hydrogen atoms are shown with arbitrarily small thermal parameters on methylene and norbornadiene groups, and are not shown for the methyl and aryl groups.

Table 4. Selected Structural Parameters for Compounds 8 and 9

atoms	$8\cdot CH_2Cl_2$	9
	Bond Lengths (Å)	
Rh(1)−P(1)	2.2514(6)	2.2642(7), 2.2590(7)[a]
Rh(2)−P(2)	2.2292(6)	
Rh(1)−N(1)	2.194(2)	2.148(2), 2.161(4)
Rh(2)−N(3)	2.205(2)	
N(1)−C(12)	1.485(3)	1.464(4), 1.456(6)
	Angles (deg)	
P(1)−Rh(1)−N(1)	84.25(5)	82.18(7), 80.84(8)
P(2)−Rh(2)−N(3)	84.16(6)	
P(1)−C(10)−P(2)	123.00(12)	
C(22)−N(2)−C(27)	110.6(2)	
C(22)−N(2)−C(28)	112.8(2)	
C(27)−N(2)−C(28)	109.6(2)	
C(42)−N(4)−C(47)	112.0(2)	
C(42)−N(4)−C(48)	111.1(2)	
C(47)−N(4)−C(48)	110.4(2)	

[a] Two crystallographically independent molecules.

indicated that the amido functionality is inert to covalent substrates (H_2 and CH_3I), and structural data provide an explanation based on resonance delocalization of amido electron density. However, these species can be readily protonated or methylated at the nitrogen atom, indicating that electrophilic addition to the amido group is possible. Conveniently, protonation of the nonlabile phosphine-amido species serves as an alternate route to hemilabile phosphine-amine complexes. The phosphine-amido complex, $[Rh(COD)(P,N\text{-}Ph_2PAr^-)]$ (**1a**), can be converted into the hemilabile phosphine-amine compound $[Rh(COD)(P,N\text{-}Ph_2PAr)][OTf]$ (**9**) by protonation with trifluoromethanesulfonic acid (HOTf). The ^{1}H NMR spectrum of **9** displays a doublet resonance for the *N*-methyl group at δ 2.62

dx.doi.org/10.1021/ic101883u |*Inorg. Chem.* 2011, 50, 5361–5378

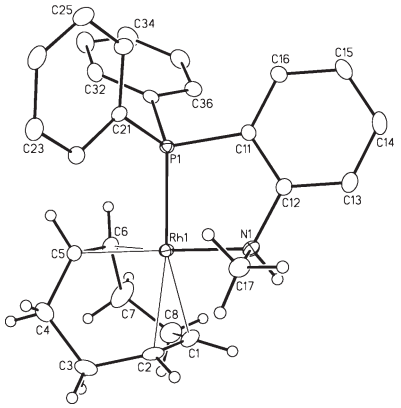

Figure 9. ORTEP Diagram of [Rh(COD)(*P*,*N*-Ph_2PAr)][OTf] (**9**). Only one of two crystallographically independent cations (A) is shown. Non-hydrogen atoms are represented by Gaussian ellipsoids at the 20% probability level. Hydrogen atoms, where shown, have been given arbitrarily small thermal parameters.

showing coupling ($^3J_{HH}$ = 6.0 Hz) with the amine hydrogen at δ 7.08, the resonance for which was identified by gCOSY analysis. In this spectrum, the COD protons appear as broad resonances suggesting fluxionality; however, a variable temperature NMR study was not undertaken in this case. The ambient temperature $^{31}P\{^1H\}$ NMR spectrum appears as a sharp doublet at δ 38.3 with $^1J_{RhP}$ = 159 Hz. This complex was isolated and characterized for proof of concept since the addition of HOTf to reaction mixtures employing amido complexes **1a**, **1b**, and **2** as catalysts (followed by passing solutions through Florisil) is a rapid and efficient means of removing catalysts from reaction mixtures. Although the reaction was not attempted, compound **9**, or its norbornadiene analogue can presumably also be synthesized directly from the corresponding *ortho*-phosphinoaniline (Ph_2PAr) and either of the cationic precursors, $[Rh(COD)_2][OTf]$ or $[Rh(NBD)_2][BF_4]$, much as outlined earlier for the synthesis of **7a**.

The X-ray structure of phosphine-amine complex **9** (Figure 9) displays a shortened olefinic bond opposite the amine donor (C(5)−C(6) = 1.383(5) and 1.388(6) Å for the two crystallographically independent molecules) when compared with that of the parent (**1a**, 1.405(2) Å) bearing the π-donating amido group. Conversion of the amido group to an amine has also resulted in a lengthening of the Rh−N bonds of **9** (2.148(2) and 2.161(4) Å) relative to that of **1a** (2.063(1) Å), presumably because of the lack of a π-interaction with rhodium in the former, although in **9** this bond remains shorter than those of **8** (2.194(2) and 2.205(2) Å) presumably, in this case, a result of decreased steric bulk of the *N*-methylamine donor in **9** relative to those of the *N*,*N*-dimethylamine donors of **8**.

In attempts to prepare the binuclear phosphine-amine compound, $[Rh_2(NBD)_2(\mu\text{-}P,N,P',N'\text{-mapm})][BF_4]_2$ (**10**), reactions of mapm with 2 equiv of $[Rh(NBD)_2][BF_4]$ in CD_2Cl_2 were performed under a range of conditions. The major product from these reactions shows spectroscopic characteristics consistent with those expected for **10**, appearing as a second order multiplet at δ 7.0 ($^1J_{RhP}$ = 170 Hz) in the ambient temperature $^{31}P\{^1H\}$ NMR spectrum and having a signal pattern similar to the other binuclear analogues described herein (**2** and **8**) and elsewhere.[22] A similar, but less intense, broadened resonance at δ 3.7 ($^1J_{RhP}$ = 172 Hz) is also seen in this spectrum. The observation of two distinct $^{31}P\{^1H\}$ signals for **10** is similar to that observed for the *N*,*N*-dimethyl analogue (**8**; vide supra), and we again attribute the less intense, more upfield signal to a C_s-symmetric intermediate, through which the C_2-symmetric enantiomers interconvert. Interestingly, variable temperature $^{31}P\{^1H\}$ NMR analysis of **10** shows that decreasing the temperature to −80 °C results in broadening of the downfield resonance (now at δ 5.6) along with sharpening and increasing intensity of the more upfield resonance (now at δ 1.9) consistent with a temperature-dependent shift in the equilibrium concentrations of C_2- and C_s-symmetric isomers. Unfortunately, the ^1H NMR spectra, at both ambient temperature and −80 °C, show broad, unresolved signals because of the presence of several other unidentified species, which also precludes our successful isolation of **10** as an analytically pure substance. An alternate method for the preparation of $[Rh_2(NBD)_2(\mu\text{-}P,N,P',N'\text{-mapm})]^{2+}$ by protonation of **2** with 2 equiv of HOTf in dichloromethane was also attempted; however, $^{31}P\{^1H\}$ and ^1H NMR analyses produced spectra similar to those described above.

Scheme 6. Possible Products from Reaction of Triethylsilane with Styrene

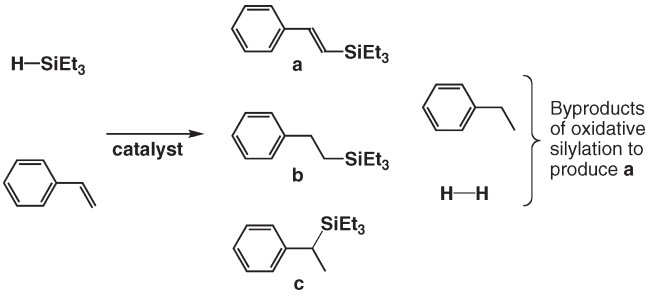

Catalytic Olefin Silylation. The complexes, [Rh(COD)(*P*,*N*-Ph_2PAr^-)] (**1a**, Ar^- = *o*-$C_6H_4NMe^-$), [Rh(COD)(*P*,*N*-PhP(Ar^-)-Ar)] (**1b**), $[Rh_2(COD)_2(\mu\text{-}P,N,P',N'\text{-}mapm^{2-})]$ (**2**), [Rh(NBD)-(*P*,*N*-Ph_2PAr')][BF_4] (**7a**), [Rh(NBD)(*P*,*N*-PhPAr'_2)][BF_4] (**7b**), and $[Rh_2(NBD)_2(\mu\text{-}P,N,P',N'\text{-dmapm})][BF_4]_2$ (**8**), which are all air stable as solids and can be isolated in good to excellent yields, were studied as catalysts for styrene silylation (Scheme 6). The spectroscopic observation of hemilability within complexes **7a**, **7b**, and **8** inspired us to compare the catalytic activities of these compounds with the nonlabile phosphine-amido analogues, **1a**, **1b**, and **2**. Specifically, we aimed to determine how the different *N*-donor functionalities might alter the rates of competing hydrosilylation and oxidative silylation processes by examining selectivities for vinylsilane **a**, and hydrosilylation products **b** and **c** (Scheme 6). Oxidative (dehydrogenative) silylation to produce **a** can occur either by direct liberation of molecular hydrogen from the reagents or by hydrogen transfer from each reagent to an additional equivalent of styrene (necessitating the use of excess styrene in reaction mixtures to promote selectivity for **a**).[11,34,35] We also wanted to examine whether or not the presence of adjacent metal atoms in the binuclear complexes would have a positive effect on reactivity (through metal−metal cooperativity)[58] by comparisons with mononuclear congeners. In addition, we sought to compare the catalytic characteristics of mononuclear compounds **1a** and **1b**, as well as **7a** and **7b**, to determine what influence the presence of an additional, pendent amine donor may have on reactivity.

The excellent solubility of the neutral amido complexes **1a**, **1b**, and **2** directly in styrene eliminated the need for any additional solvent, and indeed several reactions were performed neat in

dx.doi.org/10.1021/ic101883u |*Inorg. Chem.* 2011, 50, 5361–5378

Table 5. Catalytic Reactions of Triethylsilane and Styrene at 60 °C

entry	catalyst	Rh/$HSiEt_3$/ Styrene	t_{rxn}(min)	conversion[a]	a[a]	b[a]	c[a]	o[a]	[Rh] (mM)
1	**1a**	1:20:100	15	59	62	36	1	1	68.0
			30	100	71	27	1	1	
2	**1a**	1:100:500	30	62	61	36	3	<1	13.6
			60	100	67	30	3	<1	
3	**1a**	1:1,000:5,000	90	72	56	33	10	<1	1.36
			180	93	60	30	9	<1	
4	**1b**	1:1,000:5,000	90	54	50	36	14	<1	1.36
			180	90	64	28	8	<1	
5	**2**	1:1,000:5,000	90	40	57	42	<1	<1	1.36
			180	68	61	38	<1	<1	
6[b]	**1a**	1:1,000:5,000	120	71	67	27	<1	6	1.20
			300	100	69	27	<1	4	
7[b]	**1b**	1:1,000:5,000	120	57	58	29	1	12	1.20
			300	93	68	24	1	8	
			1,440	100	72	21	1	6	
8[b]	**2**	1:1,000:5,000	120	54	65	34	1	0	1.20
			300	79	66	33	1	0	
			1,440	100	65	32	1	2	
9[b]	**7a**	1:1,000:5,000	120	58	55	35	6	4	1.20
			300	82	58	34	4	4	
			1,440	100	64	29	3	4	
10[b]	**7b**	1:1,000:5,000	120	41	47	36	1	16	1.20
			300	84	62	28	1	9	
			1,440	100	64	26	1	9	
11[b]	**8**	1:1,000:5,000	120	40	42	20	2	36	1.20
			300	71	60	19	1	20	
			1,440	100	67	19	1	13	
12[c]	other	1:20:100	1,440	98	96	2	<1	<1	5

[a] Conversions and selectivities (%) for *E*-$Ph(CH)_2SiEt_3$ (**a**), $Ph(CH_2)_2SiEt_3$ (**b**), (±)-$PhCH(CH_3)SiEt_3$ (**c**) and other (**o**) silicon-containing products determined by GC-MS and ^1H NMR analysis on samples obtained at corresponding reaction times (t_{rxn}) in column 4. Reactions were carried out neat in styrene and triethylsilane unless indicated otherwise. [b] Reactions were carried out in the presence of 1,000 equiv of $C_6H_5NO_2$ per equiv of Rh. [c] Data obtained from ref 11; here the values reported in **a**, **b**, **c**, and **o** columns represent yields (%) rather than selectivities. Reaction was carried out in toluene.

reagents (See Table 5, Entries 1−5). Despite their excellent solubilities, rapid separation of these catalysts from reaction mixtures was made possible by protonation of the amido groups with HOTf to generate ionic species that could then be easily removed using a Florisil column. Cationic species **7a**, **7b**, and **8**, which were insoluble in styrene, were dissolved in an appropriate volume of nitrobenzene prior to reagent addition so that the mole ratio of components in the reaction mixtures was $Rh/HSiEt_3$/styrene/$C_6H_5NO_2$ = 1:1,000:5,000:1,000 in each case (Entries 9−11, respectively). These cationic phosphine-amine catalysts are readily removed from reaction mixtures (without protonation by HOTf) using a Florisil column, as described above.

At the outset, we intended to investigate the reactivities of the phosphine-amido compounds (**1a**, **1b**, and **2**), anticipating that the possibility of metal−metal cooperativity[58] might result in a rate enhancement for catalyst **2** relative to **1b**. However, a comparison of Entries 3−5 shows that both mononuclear

Chart 1. Reaction Profiles for Catalysts 1a, 1b, and 2[a]

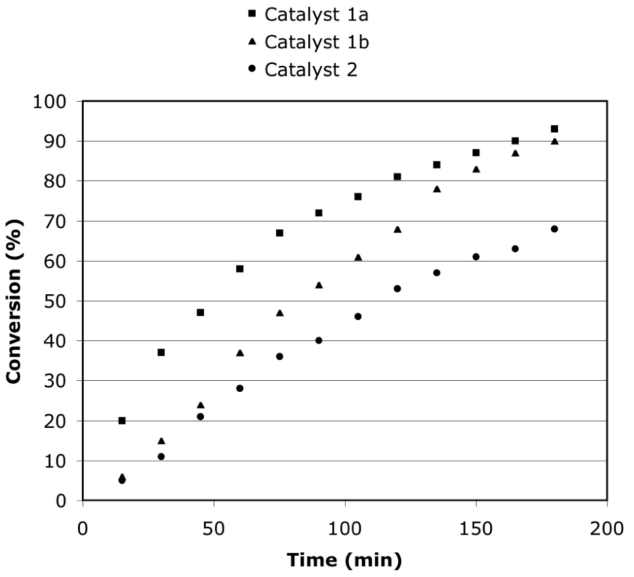

[a] Catalysts were dissolved in styrene and resultant mixtures were heated at the reaction temperature (60 °C) for 10 min prior to the addition of triethylsilane. The molar ratio of reaction components in each case was $Rh/HSiEt_3$/styrene =1:1,000:5,000. Aliquots withdrawn from reaction mixtures at 15 min intervals for 180 min were treated and analyzed as described in the Experimental Section.

complexes (**1a** and **1b**) are actually somewhat more active than **2**, indicating that the presence of two adjacent metal centers actually appears to have an adverse effect, perhaps because of crowding within the binuclear complex. Comparisons of **1a** and **1b** as catalysts (Entries 3, 4, 6, and 7) demonstrate that the presence of a pendent amine appears to result in somewhat slower initial activity, but does not seem to affect the overall activity of the complex at longer reaction times.

Entries 3−5 provide representative data obtained from a more detailed kinetic analysis of the phosphine-amido catalysts, undertaken to compare their activities at predetermined intervals as reactions progressed (see Chart 1). A comparison of the reaction profiles shows superior activity of **1a** over both **1b** and **2** at early stages of the reaction; however, as reactions approach completion, the activity of **1a** slows noticeably relative to that of **1b**. The initially slower conversion of silane observed for **1b** relative to **1a** is consistent with the presence of the pendent amine in **1b** competing with substrates for coordination to rhodium, rendering the active site of **1a** more accessible. However, the more gradual conversion of silane observed for **1b** suggests that, in this case, catalyst decomposition is slowed by the provision of a hemilabile donor to rhodium, thereby stabilizing catalytic intermediate(s) in the event of coordinative unsaturation at the metal. A comparison of the activities of **1b** and **2** illustrates that at the initial stages of the reaction, the two are comparable. However, as the reactions proceed, the activity of **2** declines to a greater extent, presumably because of faster decomposition of the binuclear analogue. The lack of a noticeable induction period in each case suggests that homogeneous catalysis by molecular species predominates under these conditions since induction periods are often observed when molecular systems decompose over time to form more catalytically active, colloidal species.[59,60]

dx.doi.org/10.1021/ic101883u |*Inorg. Chem.* 2011, 50, 5361–5378

To compare the neutral and cationic species as catalysts under identical conditions, reactions were initially carried out in the presence of nitromethane, in which the cationic species are soluble. However, we find that the phosphine-amido series is unstable in the presence of this Brønsted acidic solvent (pK_a = 10.2),[61] resulting in decomposition of these catalysts at the reaction temperature. For example, heating **1a** to 60 °C for 3 h in the presence of 10 equiv of CH_3NO_2 in C_6D_6 reveals decomposition to at least four other species as indicated by $^{31}P\{^1H\}$ NMR analysis. In nitrobenzene, however, compounds **1** and **2** are quite stable at the reaction temperature, as shown by $^{31}P\{^1H\}$ NMR spectra of the compounds obtained after 3 h at 60 °C. Nitrobenzene was therefore chosen as a common solvent for each of the catalysts to make more meaningful comparisons between the amido- and amine-containing species. An analysis of Table 5 (Entries 6−11) shows that the neutral phosphine-amido catalysts are more active than their cationic phosphine-amine counterparts, possibly because of greater propensity for silane oxidative addition by the former series containing the more electron-rich metal centers. Consistent with the trends discussed above for the phosphine-amido series, a comparison of Entries 9−11 in Table 5 shows that the phosphine-amine catalyst **7a** exhibits enhanced initial reactivity relative to **7b**, bearing the pendent amine donor, and that as reactions approach completion, the activities of these species are comparable. Again, the binuclear complex (**8**) is shown to be the least active catalyst within this series.

During each of the reactions detailed in Table 5, initially orange reaction mixtures quickly became lighter in color upon the addition of triethylsilane, followed by eventual darkening of the color at or near complete conversions, effectively signaling the end of a reaction. In general, it was noticed that more gradual darkening of solution colors correlated with slower, more steady conversions of triethylsilane. This darkening of solution colors as reactions progress, along with the change in product selectivity that is observed during the course of any given reaction, seems to indicate some degree of catalyst decomposition over time. Unfortunately, the low concentrations of catalysts used in reaction mixtures precluded NMR spectroscopic analyses of rhodium-containing species remaining after reactions were stopped.

The complexes studied show comparable selectivities for vinylsilane product **a** (see Scheme 6) and in general, selectivities for this product are found to increase slightly as reactions progress, suggesting that the catalysts may undergo transformation(s) as the number of turnovers increases, resulting in variable product distributions that depend on the extent of reaction. Entry 12 shows catalytic data for the reaction reported by Stradiotto et al., which was carried out using an analogous zwitterionic *P,N*-catalyst lacking the amido functionality.[11] Although our complexes appear to be more active than this zwitterionic catalyst, as made evident by significantly lower catalyst loadings (compare Entries 6−11 with 12) and faster conversions in our case, the latter is shown to be far more selective for unsaturated organosilane, **a**.

We suggest that the phosphine-amido complexes achieve silane activation by oxidative addition rather than by invoking reactivity of the amido group since the reaction of iodomethane with **3** shows that the polar covalent substrate prefers oxidative addition at rhodium—certainly the phosphine-amine complexes must activate the silane in such a manner. Interestingly, CG-MS data from every reaction reported in Table 5 indicates that significantly less of the hydrogen transfer byproduct, ethylbenzene, is produced than **a** (often less than 50% (mol/mol)). Such an observation implies the role of a process involving direct liberation of molecular hydrogen from reaction mixtures in addition to loss of hydrogen via hydrogenation of excess styrene. Each of the catalysts generally favors *anti*-Markovnikov regiochemistry and there is no evidence for the unsaturated products *Z*-$Ph(CH)_2SiEt_3$ or $PhC(SiEt_3)=CH_2$ in any of the reaction mixtures analyzed in this study. However, small quantities of $O(SiEt_3)_2$ were often identified among the products, presumably because of the presence of adventitious water in reaction mixtures.

The addition of stoichiometric quantities of various silanes (including, $HSiEt_3$, $HSi(OEt)_3$, $HSiPh_3$, and H_2SiPh_2) to compound **1a** in the absence of olefinic reagents results in very slow reactivity, often over a few days at ambient temperature, or over a period of hours at 60 °C, consistently and gradually decomposing to afford complex mixtures of multiple products as observed by $^{31}P\{^1H\}$ and ^1H NMR spectroscopy. The halosilanes $ClSiEt_3$ and $ISiMe_3$ also react with **1a**, albeit more readily, to produce complex mixtures. Complexes **1a**, **1b**, and **2** are each stable in the presence of excess styrene per equiv of rhodium at 60 °C for 3 h as judged by NMR analyses. The amido complex, [Rh(*P,P*′-dppe)(*P,N*-Ph_2PAr^-)] (**3**), was not tested as a catalyst since it failed to react with triethyl-, triphenyl-, or diphenylsilanes in refluxing tetrahydrofuran. However, this compound was found to react exothermically upon the addition of 1 equiv of phenylsilane at ambient temperature, generating a yellow solution composed of many spectroscopically unidentifiable species. The reactivity of **3** with the monosubstituted silane could make this complex suitable for a catalytic application similar to that described above. However, such an investigation was not undertaken during this study.

CONCLUSIONS

A new series of mono- and binuclear rhodium complexes containing anionic or neutral *P,N*-ligands has been prepared. Deprotonation of phosphine-amine ligands, Ph_2PAr, $PhPAr_2$ or $Ar_2PCH_2PAr_2$, by the base-containing precursor, $[Rh(\mu\text{-OMe})(COD)]_2$, generates the phosphine-amido complexes [Rh(COD)(*P,N*-Ph_2PAr^-)] (**1a**), [Rh(COD)(*P,N*-$Ph_2P(Ar^-)Ar$)] (**1b**), or $[Rh_2(COD)_2(\mu\text{-}P,N,P',N'\text{-mapm}^{2-})]$ (**2**), respectively. Replacement of the cyclooctadiene functionality of **1a** with 1,2-bis(diphenylphosphino)ethane (dppe) yields [Rh(*P,P*′-dppe)(*P,N*-Ph_2PAr^-)] (**3**) while protonation of **1a** with HOTf occurs at nitrogen to produce [Rh(COD)(*P,N*-Ph_2PAr)]][OTf] (**9**). Displacement of a diolefin ligand in $[Rh(NBD)_2][BF_4]$ by the phosphine-amine ligands, Ph_2PAr', $PhPAr'_2$, dmapm, or mapm produces the hemilabile compounds $[Rh(NBD)(P,N\text{-}Ph_2PAr')][BF_4]$ (**7a**), $[Rh(NBD)(P,N\text{-}PhPAr'_2)][BF_4]$ (**7b**), $[Rh_2(NBD)_2(\mu\text{-}P,N,P',N'\text{-dmapm})][BF_4]_2$ (**8**), and $[Rh_2(NBD)_2(\mu\text{-}P,N,P',N'\text{-mapm})][BF_4]_2$ (**10**), respectively.

A comparison of the structures of amido and amine complexes shows the expected planarity at the amido nitrogen, as well as shorter Rh−N bond lengths in the amido complexes. However, these species also display shorter N-aryl bonds and variations in the C−C bond lengths within the aryl group that are consistent with delocalization of the amido lone pair over the aromatic ring, which has significant chemical implications as demonstrated by the lack of reactivity of phosphine-amido complex **3** with H_2. The electron-withdrawing effect of the aryl group at nitrogen renders

dx.doi.org/10.1021/ic101883u |*Inorg. Chem.* 2011, 50, 5361–5378

the lone pair unavailable for heterolytic activation of H_2, while also lowering the basicity of rhodium, effectively preventing H_2 oxidative addition at the metal. However, compound **3** does readily undergo oxidative additions of O_2 and CH_3I to give the expected Rh(III) products, $[RhO_2(P,P'\text{-dppe})(P,N\text{-}Ph_2PAr^-)]$ (**4**) and $[RhI(CH_3)(P,P'\text{-dppe})(P,N\text{-}Ph_2PAr^-)]$ (**5**), respectively. Attempts to induce 1,2-methyl migration from rhodium to the amido nitrogen in the iodo/methyl product **5** were unsuccessful, although direct methylation at nitrogen is observed upon reaction of **3** with Me_3OBF_4, to generate $[Rh(P,P'\text{-dppe})(P,N\text{-}Ph_2PAr')][BF_4]$ (**6**). Protonation of **3** also yielded a phosphine-amine product at ambient temperature. Surprisingly perhaps, low temperature protonation suggests greater nucleophilicity of the aryl group, with subsequent proton migration to nitrogen upon warming; certainly no sign of protonation at Rh was observed.

The neutral phosphine-amido complexes were found to be more active as silylation catalysts than the cationic phosphine-amine derivatives, and although it was anticipated that the binuclear complexes might exhibit metal−metal cooperativity effects with respect to catalytic activity or selectivity, a comparison of these species with their mononuclear congeners shows that the binuclear complexes are less effective catalysts. These observations contrast the reactivity displayed by tetraphosphine complexes, which were found to be more active as hydroformylation catalysts than their mononuclear analogues, presumably as a result of metal−metal cooperativity.[58] The presence of pendent amine donors within the catalysts was found to result in more steady conversions to products, and it appears that catalyst decomposition is inhibited relative to species lacking these groups, suggesting that the addition of a pendent hemilabile functionality to a catalyst may enhance its robustness; these results may have important implications for the design of more effective catalyst systems. While the complexes studied are quite active as catalysts for the dehydrogenative silylation of styrene favoring a single unsaturated product, none of the catalysts studied exhibited excellent selectivity for this vinylsilane. The neutral phosphine-amido complexes were exceedingly soluble in styrene, negating the need for a solvent in reaction media, and could be easily removed from product mixtures by protonation to afford the cationic phosphine-amine species.

Although the phosphine-anilido complexes described in this paper display interesting reactivity, including their catalytic activity, the modulating influence of the aryl group attached to the amido nitrogen suggests that their reactivity will differ significantly from that of the alkyl-amido complexes conventionally used in "outer-sphere" transfer hydrogenation catalysis. In our case, the electron-withdrawing character of the aryl group at nitrogen, in combination with a relatively electron-rich Rh(I) center results in the apparent nucleophilicity of the arene upon protonation, which contrasts the previously demonstrated electrophilicity of the anilido ligand within an electron-poor Os(IV) complex.[62]

■ ASSOCIATED CONTENT

Ⓢ Supporting Information. Tables of crystallographic experimental details for compounds **1a**·C_6H_6, **2**·C_4H_8O, **3**·C_4H_8O, **4**·2.5C_6H_6, **5**·$C_4H_{10}O$·2C_4H_8O, **8**·CH_2Cl_2, and **9**, and selected bond lengths within the pendent methylanilinyl group in compound **2** and within the phosphine-amido ligands of compounds **3**, **4**, and **5** in pdf format. Atomic coordinates, interatomic distances and angles, anisotropic thermal parameters and hydrogen parameters for these compounds in a CIF file. This material is available free of charge via the Internet at http://pubs.acs.org.

■ AUTHOR INFORMATION

Corresponding Author

*E-mail: martin.cowie@ualberta.ca. Fax: 01 7804928231. Phone: 01 7804925581.

■ ACKNOWLEDGMENT

We thank the Natural Sciences and Engineering Research Council of Canada (NSERC) and the University of Alberta for financial support for this research and for providing two Queen Elizabeth II Graduate Scholarships to L.J.H. We thank NSERC for funding the Bruker D8/APEX II CCD diffractometer and the Nicolet Avatar IR spectrometer. We thank the Department's Analytical and Instrumentation Laboratory, NMR Spectroscopy Laboratory and Mass Spectrometry Facility for exceptional assistance, and M. E. Slaney for supplying a sample of $[D(OEt_2)_2][BAr^F{}_4]$.

■ REFERENCES

(1) Keim, W.; Kowaldt, F. H.; Goddard, R.; Krüger, C. *Angew. Chem., Int. Ed. Engl.* **1978**, *17*, 466–467.
(2) Braunstein, P.; Naud., F.; Rettig, S. J. *New J. Chem.* **2001**, *25*, 32–39.
(3) Holz, J.; Kadyrov, R.; Borns, S.; Heller, D.; Börner, A. *J. Organomet. Chem.* **2000**, *603*, 61–68.
(4) Shirakawa, E.; Kurahashi, T.; Yoshida, H.; Hiyama, T. *Chem. Commun.* **2000**, 1895–1896.
(5) Yang, H.; Alvarez-Gressier, M.; Lugan, N.; Mathieu, R. *Organometallics* **1997**, *16*, 1401–1409.
(6) Espinet, P.; Soulantica, K. *Coord. Chem. Rev.* **1999**, *193 − 195*, 499–556.
(7) Gunanathan, C.; Ben-David, Y.; Milstein, D. *Science* **2007**, *317*, 790–792.
(8) Maire, P.; Büttner, T.; Breher, F.; Le Floch, P.; Grützmacher, H. *Angew. Chem., Int. Ed.* **2005**, *44*, 6318–6323.
(9) Lundgren, R. J.; Rankin, M. A.; McDonald, R.; Schatte, G.; Stradiotto, M. *Angew. Chem., Int. Ed.* **2007**, *46*, 4732–4735.
(10) Lundgren, R. J.; Stradiotto, M. *Chem.—Eur. J.* **2008**, *14*, 10388–10395.
(11) Cipot, J.; McDonald, R.; Ferguson, M. J.; Schatte, G.; Stradiotto, M. *Organometallics* **2007**, *26*, 594–608.
(12) Jeffrey, J. C.; Rauchfuss, T. B. *Inorg. Chem.* **1979**, *18*, 2658–2666.
(13) Braunstein, P.; Naud, F. *Angew. Chem., Int. Ed.* **2001**, *40*, 680–699.
(14) Lindner, E.; Pautz, S.; Haustein, M. *Coord. Chem. Rev.* **1996**, *155*, 145–162.
(15) Slone, C. S.; Weinberger, D. A.; Mirkin, C. A. *Prog. Inorg. Chem.* **1999**, *48*, 233–350.
(16) Werner, H. *Dalton Trans.* **2003**, 3829–3837.
(17) Bassetti, M. *Eur. J. Inorg. Chem.* **2006**, 4473–4482.
(18) Jones, N. D.; James, B. R. *Adv. Synth. Catal.* **2002**, *344*, 1126–1134.
(19) Foo, S. J. L.; Jones, N. D.; Patrick, B. O.; James, B. R. *Chem. Commun.* **2003**, 988–989.
(20) Jones, N. D.; Foo, S. J. L.; Patrick, B. O.; James, B. R. *Inorg. Chem.* **2004**, *43*, 4056–4063.
(21) Jones, N. D.; Meessen, P.; Losehand, U.; Patrick, B. O.; James, B. R. *Inorg. Chem.* **2005**, *44*, 3290–3298.

(22) Hounjet, L. J.; Bierenstiel, M.; Ferguson, M. J.; McDonald, R.; Cowie, M. *Dalton Trans.* **2009**, 4213–4226.
(23) Fernández-Galán, R.; Jalón, F. A.; Manzano, B. R.; Rodríguez-de-la-Fuente, J.; Vrahami, M.; Jedlicka, B.; Weissensteiner, W.; Jogl, G. *Organometallics* **1997**, *16*, 3758–3768.
(24) Bertini, I.; Dapporto, P.; Fallani, G.; Sacconi, L. *Inorg. Chem.* **1971**, *10*, 1703–1707.
(25) Baker, K. V.; Brown, J. M.; Cooley, N. A.; Hughes, G. D.; Taylor, R. J. *J. Organomet. Chem.* **1989**, *370*, 397–406.
(26) Hounjet, L. J.; Bierenstiel, M.; Ferguson, M. J.; McDonald, R.; Cowie, M. *Inorg. Chem.* **2010**, *49*, 4288–4300.
(27) Bacchi, A.; Balordi, M.; Cammi, R.; Elviri, L.; Pelizzi, C.; Picchioni, F.; Verdolino, V.; Goubitz, K.; Peschar, R.; Pelagatti, P. *Eur. J. Inorg. Chem.* **2008**, 4462–4473.
(28) Liang, L.-C.; Chien, P.-S.; Huang, M.-H. *Organometallics* **2005**, *24*, 353–357.
(29) Huang, M.-H.; Liang, L.-C. *Organometallics* **2004**, *23*, 2813–2816.
(30) Gao, J.-X.; Ikariya, T.; Noyori, R. *Organometallics* **1996**, *15*, 1087–1089.
(31) Haack, K.-J.; Hashiguchi, S.; Fujii, A.; Ikariya, T.; Noyori, R. *Angew. Chem., Int. Ed. Engl.* **1997**, *36*, 285–288.
(32) Casey, C. P.; Johnson, J. P. *J. Org. Chem.* **2003**, *68*, 1998–2001.
(33) Clapham, S. E.; Hadzovic, A.; Morris, R. H. *Coord. Chem. Rev.* **2004**, *248*, 2201–2237.
(34) Takeuchi, R.; Yasue, H. *Organometallics* **1996**, *15*, 2098–2102.
(35) Kakiuchi, F.; Nogami, K.; Chatani, N.; Seki, Y.; Murai, S. *Organometallics* **1993**, *12*, 4748–4750.
(36) Zhang, Z.; Sherlock, D.; West, R.; West, R. *Macromolecules* **2003**, *36*, 9176–9180.
(37) Fritz, H. P.; Gordon, I. R.; Schwarzhans, K. E.; Venanzi, L. M. *J. Chem. Soc.* **1965**, 5210–5216.
(38) Jones, N. D.; Meessen, P.; Smith, M. B.; Losehand, U.; Rettig, S. J.; Patrick, B. O.; James, B. R. *Can. J. Chem.* **2002**, *80*, 1600–1606.
(39) Uson, R.; Oro, L. A.; Cabeza, J. A. *Inorg. Synth.* **1985**, *23*, 126–130.
(40) Programs for diffractometer operation, unit cell indexing, data collection, data reduction, and absorption correction were those supplied by Bruker.
(41) Altomare, A.; Burla, M. C.; Camalli, M.; Cascarano, G. L.; Giacovazzo, C.; Guagliardi, A.; Moliterni, A. G. G.; Polidori, G.; Spagna, R. *J. Appl. Crystallogr.* **1999**, *32*, 115–119.
(42) Sheldrick, G. M. *Acta Crystallogr.* **2008**, *A64*, 112–122.
(43) Beurskens, P. T.; Beurskens, G.; de Gelder, R.; Smits, J. M. M; Garcia-Granda, S.; Gould, R. O. *The DIRDIF-2008 program system*; Crystallography Laboratory, Radboud University: Nijmegen, The Netherlands, 2008.
(44) Zefirov, Y. V.; Zorkii, P. M. *Russ. Chem. Rev. (Engl. Transl.)* **1989**, *58*, 421–440.
(45) Bruice, P. Y. *Organic Chemistry*, 4th ed.; Pearson: Upper Saddle River, NJ, 2004; p 271.
(46) Dahlenburg, L.; Herbst, K.; Zahl, A. *J. Organomet. Chem.* **2000**, *616*, 19–28.
(47) Bacon, G. E. *Acta Crystallogr.* **1951**, *4*, 558–561.
(48) Lebel, H.; Ladjel, C.; Bélanger-Gariépy, F.; Schaper, F. *J. Organomet. Chem.* **2008**, *693*, 2645–2648.
(49) Vaska, L. *Science* **1963**, *140*, 809–810.
(50) Fryzuk, M. D.; MacNeil, P. A.; Rettig, S. J. *Organometallics* **1986**, *5*, 2469–2476.
(51) Feliz, M.; Freixa, Z.; van Leeuwen, P. W. N. M.; Bo, C. *Organometallics* **2005**, *24*, 5718–5723.
(52) Gunanathan, C.; Ben-David, Y.; Milstein, D. *Science* **2007**, *317*, 790–792.
(53) Brookhart, M.; Grant, B.; Volpe, A. F., Jr. *Organometallics* **1992**, *11*, 3920–3922.
(54) Dorta, R.; Shimon, L.; Milstein, D. *J. Organomet. Chem.* **2004**, *689*, 751–758.
(55) Allred, A. L. *J. Inorg. Nucl. Chem.* **1961**, *17*, 215–221.
(56) Huheey, J. E. *J. Phys. Chem.* **1965**, *69*, 3284–3291.
(57) (a) Bent, H. A. *J. Chem. Phys.* **1959**, *33*, 1258–1259. (b) Bent, H. A. *Chem. Rev.* **1961**, *61*, 275–311. (c) Alabugin, I. V.; Manoharan, M.; Buck, M.; Clark, R. J. *J. Mol. Struct. THEOCHEM* **2007**, *813*, 21–27.
(58) Broussard, M. E.; Juma, B.; Train, S. G.; Peng, W.-J.; Laneman, S. A.; Stanley, G. S. *Science* **1993**, *260*, 1784–1788.
(59) Lewis, L. N.; Lewis, N. *J. Am. Chem. Soc.* **1986**, *108*, 7228–7231.
(60) Stein, J.; Lewis, L. N.; Gao, Y.; Scott, R. A. *J. Am. Chem. Soc.* **1999**, *121*, 3693–3703.
(61) Murata, K.; Konishi, H.; Ito, M.; Ikariya, T. *Organometallics* **2002**, *21*, 253–255.
(62) Soper, J. D.; Saganic, E.; Weinberg, D.; Hrovat, D. A.; Benedict, J. B.; Kaminsky, W.; Mayer, J. M. *Inorg. Chem.* **2004**, *43*, 5804–5815.